MASTER'S THESIS 2019

Kinetic Modelling of Fluidised Bed Drying of Enzyme Granules and Effect on Shelf-Life Stability

Edvin Ingmarsson

DEPARTMENT OF BIOTECHNOLOGY
LTH | LUND UNIVERSITY

Abstract

In the production of solid enzyme products, the granules are dried in a fluidised bed dryer prior to being coated with a protective salt coating. The coating exhibits a low mass diffusivity, which essentially encapsulates any present moisture inside. During the coating process moisture is inevitably added to the granules. It has prior been shown that moisture content in the final product has a negative impact on the shelf-life stability of some of the enzyme product produced by Novozymes. It has been theorised whether it is the moisture of the granules before the coating is applied, or the moisture added during the coating which accounts for this effect. The primary objective in this thesis was to determine the correlation between moisture content from the dryer and the final products shelf-life stability. From experimental data a clear correlation was observed. A considerably decrease in absolute enzyme activity was observed when the coating was performed with high moisture content granules. It is thought that high moisture content combined with a high temperature cause the enzymes to denature. Furthermore a mathematical model was implemented in Python to simulate the drying. The simulations were shown to predict the moisture content of the granules well to the experimental data. However the simulated temperatures deviates considerably from measured values.

Keywords: fluidised bed, drying, enzyme, stability, mathematical modelling

Acknowledgements

This master dissertation finalises my Master of Science in Chemical Engineering. The thesis was carried out at Division of Biotechnology at Lund University, Faculty of Engineering.
I would like to thank assisting supervisor Dr. Pär Tufvesson at Novozymes for feedback, valuable discussions and guidance throughout the project. Furthermore I would like to send my gratitude to Dr. Carl Grey and Prof. Patrick Adlercreutz for supervision and providing feedback.
Without the help of the co-workers at Novozymes this project would not have been possible. Great thanks to pilot technician Tonny Damgaard with performing the drying experiments, laboratory technician Martin Mellergaard for guidance with laboratory work and Maria Ellehammer Del Risco for the 'do and don't' in the lab. Thank you everyone at SPD for welcoming me during the work.

Bagsværd, September 2019
Edvin Ingmarsson

Contents

1

Introduction

This first chapter contains a brief introduction to the phenomena of fluidised beds, its history and applications. In addition the utilisation of fluidised drying beds in production of enzyme granules is discussed. The chapter is finalised with the objectives and the outline of the thesis.

1.1 Background

Fluidised beds is a frequently used unit operation in multiple industries, with the most prominent being pharmaceuticals [1], biotechnology [2], metallurgy, semiconductors, polymers & agriculture. The excellent heat and mass transfer which is obtained in a fluidised bed make it a useful technology both for reaction and drying utilisations. Fluidisation is the phenomena when solid particles obtain a fluid-like state when suspended in a up flow of air or liquid. The obtained state shows some highly unusual characteristics – with different properties and behaviours depending on the flow rate of the liquid or air.
The first large scale commercial application of fluidised beds was as early as 1926, the Winkler's coal gasifier. Due to the eminent threat of World War II to Europe and the Far East, USA predicted that the demand for aviation fuel would drastically increase, causing an acceleration of the development effort of the fluidised bed technology. In the early 1940's the predecessor to Exxon had developed and built the first fluid catalytic cracking (FCC) unit – entering smooth operation in 1942 dramatically increasing the production capacity of aviation fuel in the US. FCC is still today the most important value increasing conversion process in petroleum refineries. The potential of fluidised beds in other industries were immediately recognised and development for additional applications of the technology began. Independently of each other the US based *Dorr-Oliver Company* and the German *Badische Anilin und Soda-Fabrik* in the middle of 1940's both began development of systems for noncatalytic gas-solid reactions. [3]
The fluidised bed dryer (FBD) is suitable for the drying of any solid given that it can be fluidised by hot air. Various designs of FBD's exists fulfilling the need for different purposes and applications – large and crude for drying of coal or small, efficient and precise for pharmaceuticals, which require precise temperatures and residence time.
The Danish based biotechnology company Novozymes A/S is a world leading producer of enzymes for industrial applications. In the manufacturing process of solid

enzyme products at Novozymes the semi-wet enzyme granules created in the granulation are dried in a fluidised bed dryer before a protective salt coating is applied. The coating is continuously sprayed on to the granules in a consecutive fluidised bed coater. During the coating, water is inevitably added to the particles and as the coating dries the diffusion rate of encapsulated moisture is severely restricted, essentially locking it inside. Some enzymes produced by Novozymes has prior been observed to exhibit a decreased shelf-life enzymatic stability when containing significant moisture contents.
One hypothesis proposed by Novozymes is that it is the moisture which is added to the granules during the coating process with causes a negative impact on the enzyme shelf-life stability. Under such outcome resources in the time-consuming drying could be saved and the production capacity improved. An alternative hypothesis is that it is the moisture content of the granules before the coating is applied which is the primary source of the effect on the stability. Then it is of interest to determine to which extent the granules have to be dried to avoid a decreased shelf-life stability.

1.2 Objectives

The primary objective of this master thesis is to investigate the correlation between moisture content of granules from the dryer and the enzyme stability. If the enzyme stability is shown to be highly dependent on the moisture content from the dryer it is of interest to be able to mathematically model and simulate the process. In addition the process parameters effect on the drying kinetics will investigated.
The aim of the thesis will be reached by the objectives:

- Determine if there is a correlation between enzyme stability and moisture content of granules from the dryer.
- Develop a mathematical model for simulation of drying in an fluidised drying bed.
- Optimise the process to improve enzymatic shelf-life of products.

2

Enzymes and Granule Production

In this chapter the production process of granulated solids enzyme products is described. The purpose is to describe the properties of the material which enters the fluidised bed dryer and the subsequent treatment of the solids. In addition a short review of enzymes, their properties and their mechanism is given. Hence the reasoning behind the hypothesis of possible correlation between enzymatic shelf-life stability and the moisture content from the dryer can be further explained. The chapter is finalised by explaining the experimental procedure to measure the enzyme stability.

2.1 Production Process

In this section the general production process of granulated solid products at Novozymes is explained. Limitations will be applied to only describe operations which are relevant for the thesis. Hence neither upstream production of enzymes, e.g. fermentation and recovery, nor other downstream treatments to the granules is described. In Figure 2.1 below a simplified flow-sheet of a typical production process for granulation of solid enzyme products is visualised.

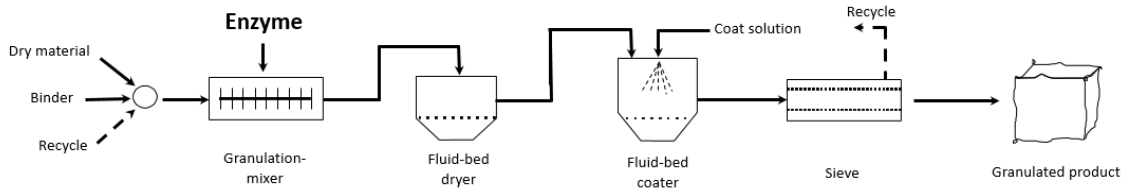

Figure 2.1: Simplified flow-sheet of a typical production process of granulated products. Adapted from internal Novozymes resources with permission.

2.1.1 Granulation

A significant risk with solid enzyme products is the capability for the enzymes to become airborne. If the enzymes are readily airborne there is a significant risk of sensitisation and ultimately development of allergy to the enzyme for exposed individuals. Hence it is common that solid enzyme products are granulated to achieve improved dust properties. [4]

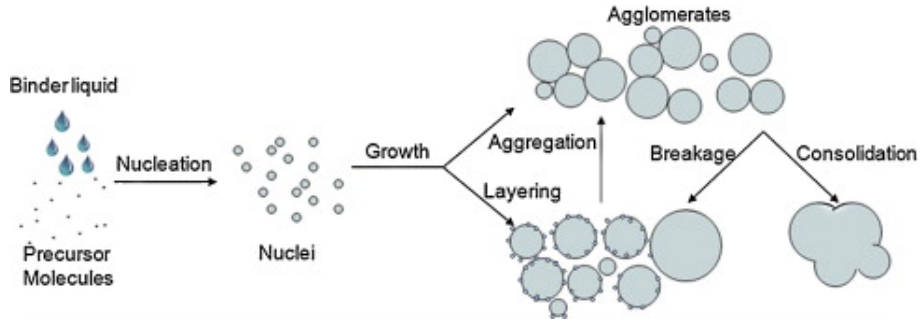

Figure 2.2: Visualisation of the phenomenons occurring in a typical wet granulation. [7]

Thus the first unit operation in the production of solid enzyme products is the granulation. Granulation is a size enlargement process in which larger particles, granules, are produced from finer materials. The granulation used in this specific application is a so called wet granulation. In Figure 2.2 the process of wet granulation is visualised. During the granulation fine particles adhere and form agglomerates held together by a binder [5]. The purpose for granulation depends on the application and industry: in the production of solid dose pharmaceuticals such as tablets and capsules granulation is performed to improve the flowability and compaction properties [6], whilst in other applications the decreased dust production of granulated product is preferred.
The enzymes are fed to a mixer together with dry raw material, downstream recycle and a binder, most often water. Additional additives may be added to the formulation to improve the characteristics of specific enzymes. In the granulation a high-shear mixer is used. The high-shear mixer ensures that the granules are compacted and hence compact and homogeneous granules of the desired size are produced.

2.1.2 Drying

After the granulation in the mixer the produced granules are emptied into the drying bed. The granules does at this point have a moisture content of about 10 % to 25 % on a dry matter basis and are rather soft. The drying of the granules is performed in a fluidised bed dryer (FBD). The principles of fluidised bed drying is explained in further detail in chapter 3. The drying is either performed in batch or continuously, depending on the production site.
Presently, the material is dried until they reach a set average temperature, which is used as an indication of how far the drying has progressed. During the drying an intermediate sieving is performed to remove granules exceeding or subceeding defined dimensions.

2.1.3 Coating

In order to protect the enzymes from the environment, e.g. harsh chemicals, the granules are given a protective coating. In addition the coating even further improves the dust properties of the final product [4]. The coating is applied to the granules in a fluidised bed coater, in which they are dried whilst simultaneously being sprayed

with a coating liquid. The exact composition of the coating liquid varies depending on the enzymes and the application, although it may essentially be described as a salt solution.
Since the salt solution is being sprayed onto the granules whilst they are being dried, a layer of salt is formed on the surface of the granules. It is this layer which protects the enzyme granules from the surrounding environment. The protective coating is essentially a complete, homogeneous layer of salt crystals which exhibit a very low mass diffusivity. Hence the process essentially encapsulates any moisture present inside the granules. It is inevitable that some additional moisture, derived from the sprayed salt solution, will be added to the granules during the coating process. During the coating process the air in the fluidised bed coater is controlled to attain a humid environment.

2.2 Enzymes and Enzymatic Stability

Enzymes are proteins which act as a catalyst in chemical reactions. Enzymes can not perform a reaction which is thermodynamically unfeasible (positive Gibbs energy) nor change the equilibrium constant. However enzymes can improve the rate of reactions. [8]
This section briefly recounts properties of enzymes and The conformational stability.

2.2.1 Enzyme Mechanisms

The active site of enzymes can bind to specific substrates – one or several at a time – and accelerates chemical reactions. Enzymes improves the reaction rate by decreasing the activation energy of the reaction, something which the enzyme can achieve by several mechanisms. Since the active site of the enzyme fits the substrate or the substrates incredibly precise it can "tear" it apart, or "force" them together. In addition, during the reaction the substrates enters one or several transition states. These transition states are characterised by exhibiting a high local maximum of free Gibbs energy and are hence unstable. The active site may conform and stabilise these transition states, and thus decreases the energy required to push the substrate over the energy barrier. [8]
Most enzymes are limited to catalyse one specific reaction, with one specific set of substrates, i.e. they exhibit a specificity. However, some enzymes have a broad specificity and can catalyse several reactions – this phenomenon is called enzyme promiscuity. The most popular way to describe how enzymes obtain their specificity was until the 60's the 'lock and key' model, created by Carl Fischer. [8]
The lock and key model suggests that the enzyme and the substrate have complementary shapes that fit each other, and can thus explain how the substrates are forced together. However, the lock and key model cannot sufficiently explain how the enzyme can stabilise the transitions states during the reaction – thus the induced fit model was developed. Since the long peptide chains in enzymes are rather flexible, Daniel Koshland suggested that the enzyme can be reshaped as it interacts with the substrates. Consequently, when the substrates bind the active site the enzyme is shaped to further improve the positioning of the active site. [9, 10]

2.2.2 Enzyme Conformational Stability Mechanisms

Due to the very specific shape of the active site, it is absolutely critical that the shape of the enzymes is not altered. The conformational stability of enzymes is dependent on the large amount of weak interactions which folds the peptide chains. At normal conditions the peptide chains of the enzymes are flexible and hence the enzyme can slightly move. At increased temperatures the flexibility of the chains increase further and the increase in movements can cause the interactions between the peptide chains to be destroyed.[11] Meanwhile water can act as an lubricant for the peptide chains, further increasing the flexibility and movements.
As the movement of the peptide chains increase the interactions which keeps the enzyme folded is not sufficient to hold the structure and the protein can unfold, or denature. When the enzyme is unfolded the function of the enzyme is lost.[11]

2.2.3 Enzyme Shelf-life Stability

Novozymes know from earlier experiments that moisture content in the final product negatively influence the shelf-life for some of the enzymes. However, one hypothesis which has been proposed is that it's the moisture which is added during the coating process will negativity influence the shelf-life stability of these enzymes – not the moisture from the fluidised bed dryer.
The reasoning is that the moisture which is added during the coating process is "locked" to the surface of the granules, unlike residual moisture from the dryer which is free to move in the bulk of the granules. As such when moisture is added to the granules during the coating, a significant moisture gradient between the surface and the bulk of the particle is created. It is theorised that it's this moisture which accounts for the decreased shelf-life stability.
The shelf-life stability of enzymes is important for Novozymes to consider since their products are commonly stored for a long period of time. In addition it is conceivable that during the transport to the customer that the product granules might be stored in unfavourable environment, i.e. high temperature and/or high humidity. The shelf-life stability thus correlates to for how long Novozymes can store the products whilst ensuring that the product is delivered on specifications to the customer with a good stability. To determine the shelf-life stability of granulated enzymes an accelerated trials can be used. The method for determination of the shelf-life stability will be further explained in subsection 5.2.2.

3

Fluidised Drying Bed

A general focal point in the thesis is fluidised bed drying. The purpose of this chapter is to introduce the phenomena of fluidisation and to further explain the process of drying solids in a fluidised bed. First a general description of fluidised bed dryers are presented. The phenomena of fluidisation is explained and discussed, and the process and kinetics associated with drying of solids in fluidised beds are presented. Phases in drying and the corresponding rate limitations are discussed.

3.1 Fluidisation

Fluidisation is a liquid-like phenomenon which a bed of solids can be observed to exhibit when a fluid is passed through the bed at sufficient rates [12]. The fluid can either be a gas or a liquid depending on the application. Fluidisation is used for many applications, not only for drying of solids, examples being: reaction engineering, catalysis, polymerisation and more [3]. When the solids are fluidised they can obtain multiple different states and the behaviours in the different states have very distinguished properties [13]. In Figure 3.1 the typical regimes which a gas fluidised bed can exhibit is visualised.
At very low fluid flow rates the fluid transfers in the interstitial space between the particles, and the properties of the bed does not significantly differ from a normal bed. A bed with these properties is called a *fixed bed*. If the flow rate is further increased the solids will begin to displace in confined regions – the bed is an *expanded bed*.
With an even further increase in flow rate the friction of upward flow of the fluid on the particles will cancel out the gravitational force of the particles, and the solids end up being suspended. This is the first state in which the bed can be described as being fluidised – the bed is at *minimum fluidisation*. An increase of the flow rate above the minimum fluidisation velocity will in a gas-solid system not create a significant additional expansion of the bed. If the suspending fluid is a liquid a increased flow rate does not produce considerable turbulence in the system, instead smooth and progressive expansion is observed. However a substantial expansion of the bed volume is observed in a liquid system.
If the bed is fluidised in a stream of air, a higher flow rate than that of the minimum fluidisation will produce instabilities in the solids, i.e. bubbles and channels of gas. At higher flow rates the turbulent behaviour of the bed can be observed to increase, with even more violent movement of solids and increased agitation. The amount of

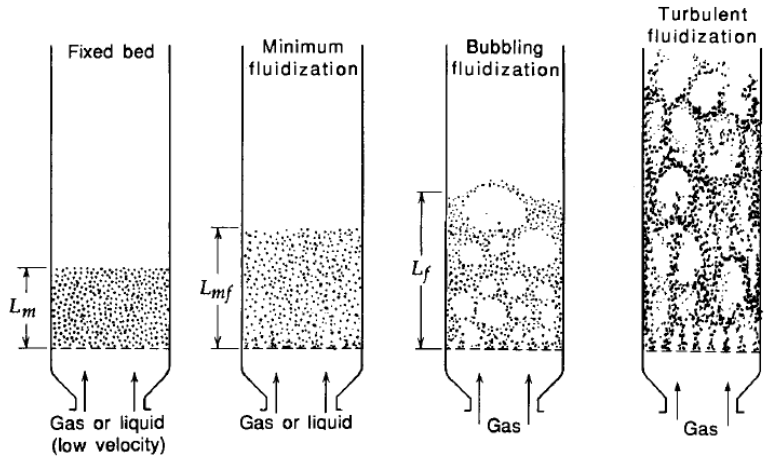

Figure 3.1: Visualisation of different regimes which can be observed in a fluidised bed at different velocities of the fluid. Adapted from [13].

bubbles in the bed will increase – the bed is at this state a *bubbling fluidised bed*. The bubbles formed at the bottom of the bed will increase in size as they ascend upwards – both due to a decreasing pressure and due to coalescence of many, smaller bubbles into fewer, larger.
The behaviour of a gas-solid system will only under specific circumstances replicate the smooth behaviour of a liquid-solid system.

3.2 Mechanisms of Drying

The drying process an air-solid system can generally be defined into three distinguishable phases. During each of the respective phases different rate limitations are effective. In a typical drying curve for a hygroscopic-porous media during constant drying conditions, three distinct phases can be observed. How the drying will progress depends both on the external conditions, i.e. air properties, equipment and flow rate, but also on internal properties, e.g. porosity, hygroscopicity & diameter [14]. This section begins by describing the stages which are observed during the drying of hypothetical ideal porous solid in a fluidised bed. This is followed by a discussion of the properties of the solid and fluid effect on the drying behaviour.

3.2.1 Stages in Drying

During each of the three periods which are observed in a typical drying curve different rate limiting phenomena influence the drying and the solids properties.

First Drying Phase: Initial Adjustment Period

The first stage in the drying process is the adjustment phase, or pre-warming. During this and the subsequent period the surface of the particle is assumed to be wet with free moisture [14]. As the air begins to fluidise the solids, the heat and mass transfer between the phases will increase. As a consequence the evaporation rate of moisture from the surface of the particles will increase – consequently energy will be removed from the solids, i.e. their temperature decreases. Meanwhile the heat transfer from

the air to the solids will increase. In essence there's an equilibrium which has to reach a steady state.
In an ideal dryer the solids surface temperature will approach the wet-bulb temperature [14]. This is due to the assumption that the evaporation interface just above the surface of the particles is completely saturated with moisture. The motivation and validity behind this assumption is discussed in the subsequent period.

Second Drying Phase: Constant Rate Period

As during the adjustment period the surface of the particles are during the constant rate period assumed to be wet with free moisture [15]. In other word the drying is limited by the evaporation rate, i.e.:

$$\boxed{\text{Evaporation rate} < \text{Internal mass transfer}}$$

The temperature of the surface of the solids will approach the wet-bulb temperature of the incoming air, T_w. This is valid under the assumption that the stagnant (assuming that film theory is valid for the particles) air just above the surface of the solids is completely saturated with moisture. Knowing the properties of the incoming air, i.e. temperature, humidity and pressure, T_w can be calculated.
The evaporation rate can during the second phase be observed to be constant – hence its name. This is valid until the internal mass transfer of moisture in the particles is not sufficient to completely wet the surface anymore. Thus the constant rate period ends when the total moisture content of the particles is lower than the threshold critical moisture content value at which the internal moisture transfer is not sufficient to completely wet the surface, a value most denoted at X_{cr}. When the moisture content is lower than X_{cr} dry spots will begin to develop and the total evaporation interface decrease – hence the evaporation rate decreases. [15]

Third Drying Phase: First Falling Rate Period

The third drying phase can be divided into two individual periods, with different kinetics limiting the drying rate in either periods. This part describes the first falling rate period.
When the content of water in the particle has decreased below the critical moisture content, X_{cr}, the internal mass transfer of water in the particle is not sufficient to completely wet the surface. Thus dry spots appear and the total evaporation interface of each individual particle decreases – the drying is now under unsaturated surface drying [14, 15]. Whilst the evaporation rate in the particle decreases, the energy transfer to the particles remain constant. Thus the solid temperature will increase. The fraction of dry surface area will throughout the phase increase, thus resulting in a gradual decreased drying rate.

$$\boxed{\text{Evaporation rate} > \text{Internal mass transfer}}$$

Depending on the physical properties of the particle, the 1st falling rate period might not be present, or constitute whole third falling rate.

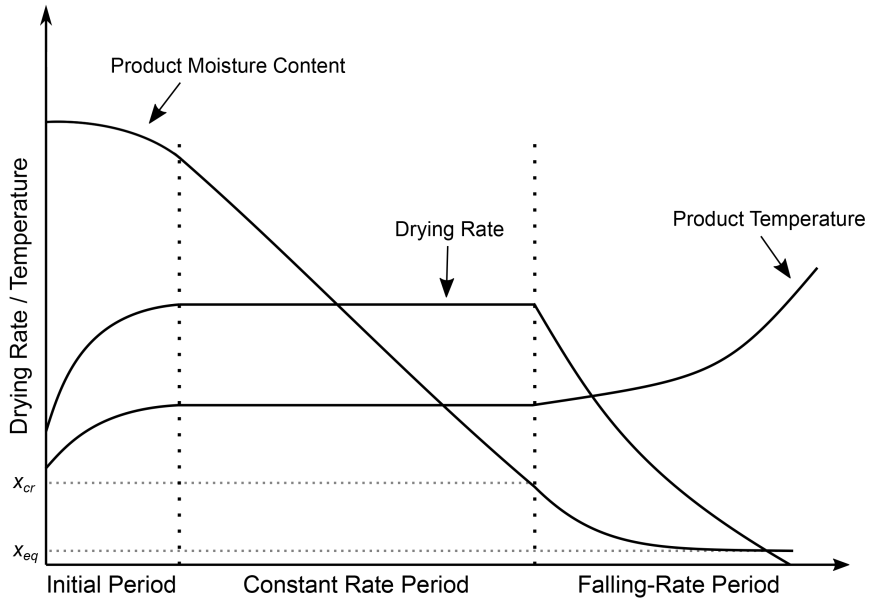

Figure 3.2: Product temperature, drying rate and moisture content of solids as a function of time in a typical drying.

Third Drying Phase: Second Falling Rate Period

As the moisture content further decreases the internal mass transfer of moisture is not sufficient to wet the surface at all, i.e.

$$\boxed{\text{Evaporation rate} \gg \text{Internal mass transfer}}$$

Thus the surface completely dries out, and the evaporation interface moves inside the particle. This results in a twofold effect – the energy is transferred by convection from the bulk air to the particle, and subsequently transferred by conductivity inside the particle. In an equal manner the evaporated moisture is transferred inside the particle to the surface of the particle, and can first then be exchanged to the bulk air. The kinetics of the transfer of the evaporated moisture inside the particle will depend on the properties of the solid. Dense, nonporous particles can be observed to be restricted to diffusion, whilst porous materials allow for capillary movement of the moisture. Consequently it can be expected that the evaporation rate of moisture will further decrease. [14]
The final moisture content which the solid is going to approach will depend both on the air and the solids properties, and is abbreviated as the equilibrium moisture content, X_{eq}. [15]

3.2.2 Drying Curve

In the prior section the stages of drying were explained. These are now combined to explain how a typical drying can be observed to progress. In Figure 3.2 a schematic illustration of the temperature and moisture content of the solids as a function of time in the dryer is presented.
Concerning the product temperature it can initially be observed to approach the wet-bulb temperature of the incoming air during the first drying phase. Depending on the initial product temperature and the air properties it can approach T_w from above

or below. The temperature is then constant throughout the constant rate period, whence after the solids temperature increases and approaches the temperature of the incoming air.
In an equal manner the evaporation rate of moisture from the solid is observed to initially increase during the pre-heating period, remain constant throughout the constant rate period and subsequently decrease during the third drying phase. Thus when observing the moisture content of the solids in the dryer as a function of time, it can initially be observed to remain approximately constant, with only a marginal decrease in moisture in the pre-heating period. During the constant rate period the moisture content decreases linearly with time, until the moisture content surpasses X_{cr} from whence the evaporation rate decreases as the surface dries out. At the end of the falling rate period the moisture content will approach X_{eq}. Additional drying will not dry the solids further unless the properties of the incoming air is altered.

3.2.3 Governing Parameters

The drying does to a rather significant extent depend on the properties of both the fluid and the solid. To accurately describe the kinetics of drying theory it is of importance that these are considered.
The properties of the solid which have a significant effect on the drying are many. The diameter of the particle is deemed to have a very large effect on the drying – not only the average diameter, but also the diameter distribution of the solids. An increase in mean diameter mean that the proportion surface area to volume is decreased, which decreases the evaporation rate. In addition, during the second falling rate period the moisture which have evaporated inside the particles will on average have a longer distance to diffuse inside the particle. Thus a dryer with particles of large diameter can be observed to have a longer drying time than one with smaller particles.
Materials can have a varying tendency to keep the moisture from evaporating from the solid, i.e. a hygroscopic property. Materials which are nonhygroscopic does not show any reluctance to the evaporation, whilst partial hygroscopic and hygroscopic can be observed to hold on to the moisture to a varying degree. [14] Further, the internal mass transfer of moisture will also play a significant role in the drying. Recalling from the earlier section, it is trivial that the moisture content at the threshold between internal and external rate limitation, X_{cr}, is a significant and governing property. This can in turn be derived to both the diameter of the solids, the materials hygroscopicity, but also the physiological characteristics of the particles. Particles which are dense and nonporous, such as sand, will mainly exhibit internal mass transfer of moisture by diffusion. Meanwhile particles which are porous will transfer moisture by capillary action. [15]
In an equal manner the specific properties of the air can be expected to influence the progress of the drying to significant degree. The moisture carrying capacity of the air is dependent on the incoming air moisture content and temperature. A higher temperature of the air increases the amount of moisture it can carry. In addition, a higher air temperature will also increase the T_w of the air, thus increasing the temperature of the solids during the constant rate period. These phenomena are best explained by visualisation in an mollier diagram. In Figure 3.3 the water carrying capacity of air in two hypothetical drying scenarios are shown. In the first drying

scenario the ambient air is 7 °C and has a relative humidity of 65 %, whilst in the other scenario the ambient air was measured at 31 °C and a relative humidity of 70 %. In both scenarios the air is heated to 45 °C and subsequently cooled adiabatically to the saturation line. As is visualised in Figure 3.3 the water carrying capacity differ significantly in the two scenarios; with the low temperature air the water carrying capacity is 0.0092 kg/kg of dry air whilst the higher temperature scenario can only saturate 0.0062 kg/kg of dry air.

3.3 Fluidised Drying

Due to the excellent heat and mass transfer in a fluidised bed the technology is suitable for drying applications. Since the bed can be observed to exhibit homogeneous temperature and moisture distribution, materials which are temperature sensitive or which require specific conditions, e.g. pharmaceuticals, the fluidised bed technology is applicable.
The technology does have some characteristics which ought to be considered when in use depending on the application. From an average residence time form of view continuous fluidised bed dryer will essentially act as an Continuous Stirred Tank Reactor (CSTR), i.e. can be observed to exhibit a distribution of the residence time of particles. The turbulent behaviour of the bed results in a mixing inside the bed, which is the cause for the residence time distribution. As a consequence consideration should be observed if the product is temperature sensitive or is required to be dried to specific conditions. This issue can be mitigated by creating 'troughs' which the solids travel along. Hence the mixing is minimised to significantly smaller gradients. An additional consequence of the turbulent behaviour of fluidised beds is the solids will repeatedly impact. Hence if the solids are friable there's a significant risk that extensive pulverisation will occur. Thus there is a risk that as the solids are pulverised into smaller parts the solids will be blown away, and result in a considerable loss of solid material. In an equal manner a considerable wear and tear on the equipment is expected if the solids are hard.

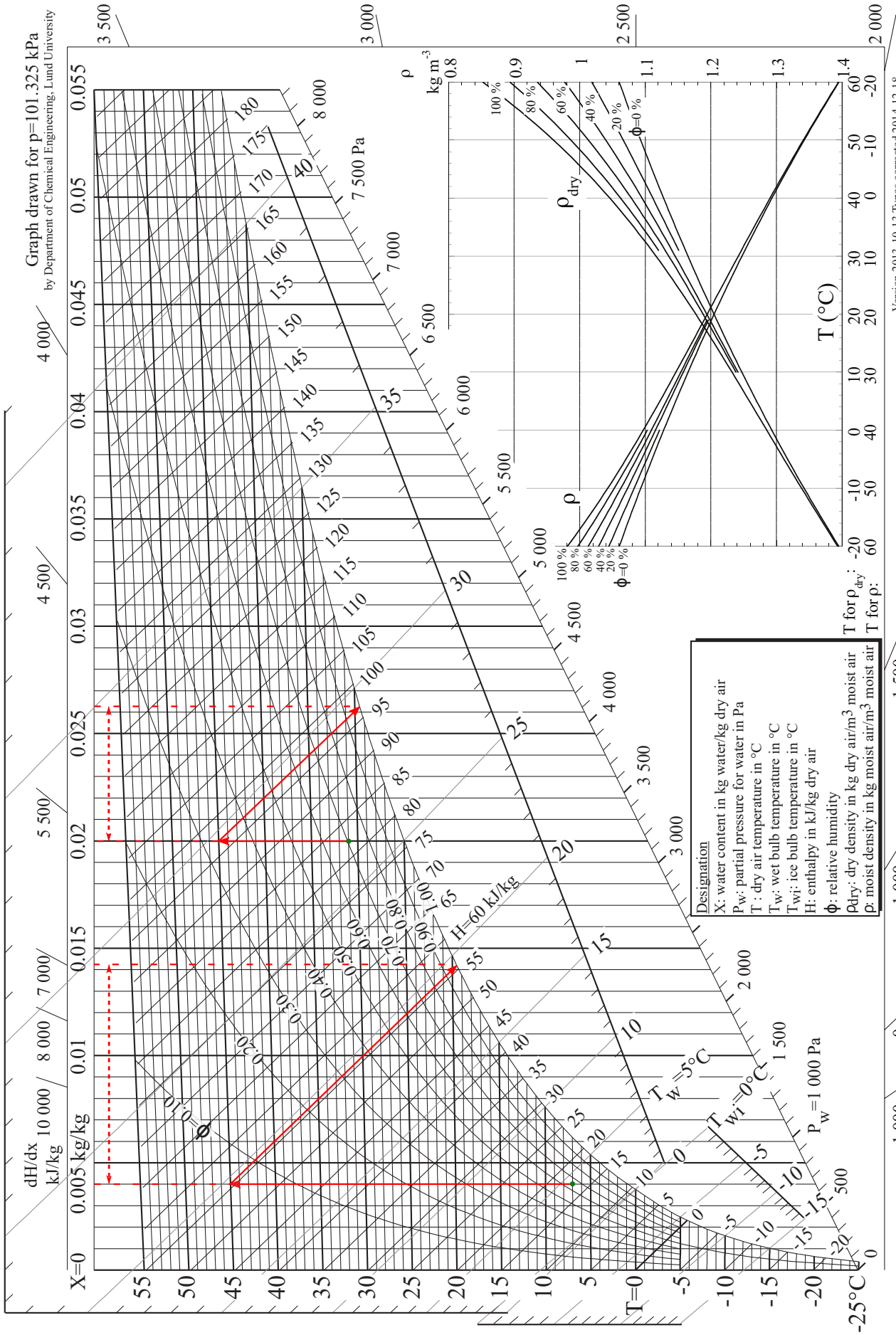

Figure 3.3: Mollier diagram visualising the water carrying capacity of air in two hypothetical scenarios. Adapted from [10]

4

Mathematical Modelling

In this chapter mathematical models for simulation of fluidised bed dryers are discussed. The chapter begins with discussing the theory behind a model which currently is the most popular to use when modelling fluidised bed dryers. The chapter is finalised with explaining the model developed as part of this thesis. The correlations which are used in the model are derived and motivated.

4.1 Kunii & Levenspiel's Three-Phase Model

The most widespread model for simulation and modelling of fluidised beds is a three-phase model which was developed by Daizo Kunii and Octave Levenspiel [16]. The model is a further development of prior work by Davidsson. Kunii and Levenspiel attempts to represent the bed by describing three different phases: bubble, cloud and emulsion.

Essentially the model describes the fluidised bed by assuming that as the bubble rise through the bed it exchanges mass with the surrounding solids. If the bubbles are large enough, a distinct layer can be observed around the bubble – the cloud phase. The cloud is assumed to move upwards with the bubble, thus the cloud phase is only present when the relative velocity of the bubble is greater than the interstitial gas velocity. Additionally it is assumed that the voidage of the solids in the cloud and emulsion phase at bubbling fluidisation is equal to the voidage at minimum fluidisation, ε_{mf}. Whilst ε_{mf} can be approximated by correlations, it is recommended to determine it experimentally at minimum fluidisation conditions. [16]

One assumption of the model is that the bubbles does not coalescence or increase in size as they ascend through the bed, instead the bubble are assumed to have a fixed diameter. In reality it has been shown that both these phenomena occur – coalescence of many smaller bubble into fewer larger has been shown to occur in beds. In addition, as the bubbles ascend though the bed, the pressure exerted on the bubble from the solids decreases, and as a results the size of the bubbles increase. The model also assumes that bubbles are perfectly spherical, however it has been shown that the bubble are round with a concave bottom.

4.1.1 Phases

In Figure 4.1 below the three different phases which Kunii and Levenspiel proposed to describe the fluidised beds are shown. In the figure the mass and energy transfers between the phases are visualised, along with the distribution of solids and gas fractions in each respective phase. The model assumes that the emulsion and cloud phase are completely homogeneous throughout the bed, whilst the bubble phase exchange mass and heat with the cloud phase as the bubble ascend the height of the bed.

Bubble Phase

The model assumes that at minimum fluidisation conditions there are no bubbles in the bed and that the emulsion phase is stagnant. Rather the complete volume of air exceeding that of minimum fluidisation is assumed to be transported through the bed as bubbles. The bubbles are assumed to transfer as a plug flow.

Cloud Phase

Around the bubble and the emulsion phase there's a thin interstitial phase, the cloud-wake phase. The cloud consist of a lower fraction solids than the emulsion phase. The fraction of cloud volume to bubble volume will decrease with a larger bubble diameter or higher bubble velocity. If the bubble velocity is very small, smaller than the interstitial gas velocity, the cloud will short cut through the bubble.

Emulsion Phase

In the model it is assumed that as the bubble rise, an upward displacement of the solids occur. As a consequence a corresponding downward transport of solids occur to counteract. Thus a continuous back-mixing occurs in the bed.

4.1.2 Attempt of Implementation

A significant effort was made in the project to reproduce Kunii and Levenspiels three-phase model to simulate a fluidised bed batch dryer in Python. The created

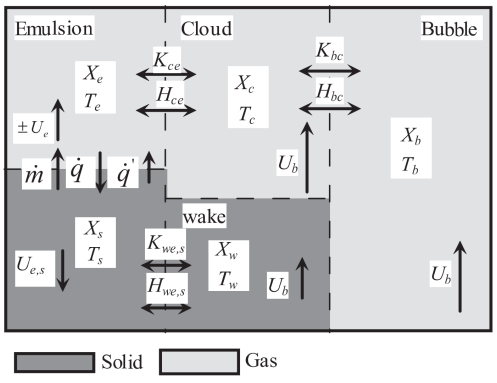

Figure 4.1: Schematic view of the phases and their interactions in the Kunii and Levenspiel model. [16]

code does not produce reasonable results. Rather, the system reaches an equilibrium at very high moisture content of the particles. Hence it is likely that an issue in the code is present. Due to time-constraints further troubleshooting was not feasible and the model was abandoned in favour of a simplified model.

4.2 General Description of Developed Model

The model which was developed in this thesis was implemented in Python. Python is an interpreted programming language which allows for quick altering of the code. The motivation behind the decision of platform is both the excellent documentation and the comprehensive libraries which are available in Python which allows for an seamless implementation. Additionally, since Python is open-source and free for commercial use it also allows for easy distribution of the developed model inside Novozymes.
The developed model strives to simulate a fluidised batch dryer by simplifying the complicated and intrinsic phenomena occurring inside the bed. Hence the model does not mechanistically describe the phenomena occurring in the bed like the three-phase model does. Rather empiric relationships are used to describe the drying process.

4.2.1 Model

In the following section the algorithm used in the model is Before the model can be initialised the operating parameters must be specified. These are as follows: Temperature and moisture content of ambient air, operating temperature and air flowrate in dryer, batch size and initial temperature of solids, enzyme type and loading. In addition the maximum humidity allowed in the dryer, denoted $\mathrm{RH_{Lim}}$.
The first step in one unit step is to calculate the kinetic rate of the granules, which is made with the function GRANULE_KINETICS. The granule kinetic rate is dependent on the moisture content of the granules at said unit step. Subsequently the wet bulb temperature of the air in the dryer at the unit step, $\mathrm{T_w}$, is calculated by WET_BULB_TEMPERATURE. With $\mathrm{T_w}$ the corresponding vapour pressure of water at the surface of the particles can be calculated and correlated to an experimentally determined kinetic rate. This step is made in TEMPERATURE_KINETICS. By combining the two kinetic rates the total driving force in the unit step, denoted as *drying_rate*, is achieved. Subsequently the driving force is fed to an ordinary differential equation which calculates the drying rate, updates the moisture content in the granules and in the air. This is done by MASS_N_HEAT_SOLVER. At very high drying rates the moisture which is removed from the granules will be greater than the amount of moisture which the air can carry, i.e. the air is supersaturated. Hence before the unit step is completed a check is performed to determine the relative humidity of the air, RELATIVE_HUMIDITY_FUNCTION. If the relative humidity exceeds an experimentally determined limit (RH_{Lim}) the calculated drying rate needs to be adjusted. If the air is calculated to be supersaturated *drying_rate* is decreased by 1 % and the calculations from MASS_N_HEAT_SOLVER are repeated until the condition is satisfied, at which point the unit step is completed.
Finally the number of unit steps performed is evaluated to the specified limit. If the number of unit steps has not reached the limit, the process returns to GRAN-

ULE_KINETICS with the new conditions. When the unit step limit is reached the code stops. In Figure 4.2 the algorithm used in the model is visualised. Figure 4.2 is a simplification, however does provide additional insights into how the functions are connected and it is hence recommended that the figure is reviewed before proceeding. In the following subsections select functions in the model are further explained and motivated:

Granule Kinetics

As was explained in section 3.2 the surface of the granules in a theoretical drying will initially be wet with free moisture. When the moisture content in the granules decrease below X_{cr} the surface will begin to dry out and the evaporation interface moves inside the granules. This causes a significant effect on the drying rate.
In the model the function GRANULE_KINETICS calculates an value based on the moisture content of the granules at the unit step. This value is used as an compensation factor to describe the earlier mentioned phenomena. GRANULE_KINETICS uses a Michaelis–Menten type of expression, as seen in Equation 4.1.

$$R = \frac{R_{max} \cdot {X_p}^n}{{K_m}^n + {X_p}^n} \tag{4.1}$$

With the constants specified as

$$R_{max} = 1 \qquad n = 2 \qquad K_m = 0.04$$

Wet Bulb Temperature Approximation

In each unit step the model calculates the wet bulb temperature, T_w, in the dryer at the conditions from the earlier unit step and uses that to approximate the vapour pressure of moisture on the surface of the granules. This is performed by the function WET_BULB_TEMPERATURE. However accurately calculating T_w from the temperature and relative humidity with a mathematical formula is a difficult task due to the complicated thermodynamics associated with the process. Hence WET_BULB_TEMPERATURE uses an empirical expression created by Roland Stull to estimate the corresponding T_w. Stull used regression of data to find an accurate expression of T_w as Equation 4.2. [17]

$$\begin{aligned} T_w \;=\; & 20 \arctan[0.151977(RH + 8.313659)^{1/2}] \\ & + \arctan(T + RH) - \arctan(RH - 1.676331) \\ & + 0.00391838(RH)^{3/2} \arctan(0.023101 \cdot RH) - 4.686035 \end{aligned} \tag{4.2}$$

In which RH for a relative humidity of 18.5 % is 18.5. This gives an approximation of the wet-bulb temperature accurate within ±1 °C from the actual T_w. The effect of the inaccuracy of T_w in WET_BULB_TEMPERATURE is deemed to be negligible, and hence the trade-off for a simplified calculations is acceptable.

Temperature Kinetic

In prior work at Novozymes a correlation between the vapour pressure at the wet-bulb temperature and the drying rate in the constant rate period was established.

In TEMPERATURE_KINETICS this correlation is used to approximate the relevant kinetics.
The wet bulb temperature of the air at the unit step which was calculated by WET_BULB_TEMPERATURE is fed to the function TEMPERATURE_KINETICS. The first step in the function is to calculate the vapour pressure of water at T_w. Equation 4.3 performs this calculation and outputs the pressure in mmHg.

$$P^0 = 10^{8.07131 - \frac{1730.63}{(T_w + 233.426)}} \tag{4.3}$$

With P^0 of water at the wet bulb temperature, the kinetic rate can be calculated to the prior mentioned correlation. From the prior work Equation 4.4 was established to satisfactory express the correlated kinetic rate during the constant rate period.

$$wet\_bulb\_rate = 0.0002 \cdot P^0 \tag{4.4}$$

Finally the *wet_bulb_rate* is multiplied with *granule_rate* which gives the *drying_rate* and hence the driving force at the unit step.

Ordinary Differential Solver

With the relevant drying kinetics in the unit step calculated in the prior operations, the mass and heat transfers on the granules can be updated. The mass and the heat transfer are connected – in the evaporation of the moisture heat is consumed, but the heat available is dependent on both the current evaporation rate and the current moisture content. Hence this operation is expressed as differential equations, as Equation 4.5 and Equation 4.6

$$\frac{dX}{dt} = -0.1 \cdot drying\_rate \tag{4.5}$$

$$\frac{dT}{dt} = \frac{T_{air\ in} \cdot c_{p,air} \cdot F - T \cdot c_{p,air} \cdot F + \frac{dX}{dt} + \Delta H_{vap} \cdot m_{solid}}{F \cdot c_{p,air} \cdot m_{solid} \cdot c_{p,salt} \cdot (1 - X) + m_{solid} \cdot X \cdot c_{p,water}} \tag{4.6}$$

In Python Ordinary Differential Equations can be solved with the help of functions available in the library SciPy. SciPy has several functions for integration of systems of ODE's. In the model the function SCIPY.CNTEGRATE.ODEINT was used to solve Equation 4.5 and Equation 4.6.

4.2.2 Parameter Fitting

In the model a numerous of parameters are used to account for the process conditions, equipment, formulation and the enzymes in the drying. These are necessary to define to accurately simulate the drying in various conditions. Properties of the air, i.e. temperature, humidity and flowrate are experimentally determined, and no fitting of these are performed. However, to account for the effect of the properties of the solids, i.e. formulation, enzyme loading and batch sie, these parameters are fitted. Moreover the relative humidity limit and the parameters of the Michaelis–Menten type expression in GRANULE_KINETICS were fitted. No effort was made to automatically fit the parameters to the experimental data. Rather a manual iterative procedure was used to determine suitable values of the parameters

at the different conditions. The experimental data acquired throughout the thesis (see chapter 6) was used in the models parameter fitting.
The validity of a manual iterative parameter fitting can be questioned. Since the model consists of numerous parameters there is an considerable possibility that inaccurate parameters can equal each other out, and thus give the impression that the values of the parameters are correct. However, in chapter 6 sensitivity analysis of single process conditions were performed. Hence the data could be used to validate the model parameters. Thus it is considered that the risk of the abovementioned phenomena is present is deemed negligible.

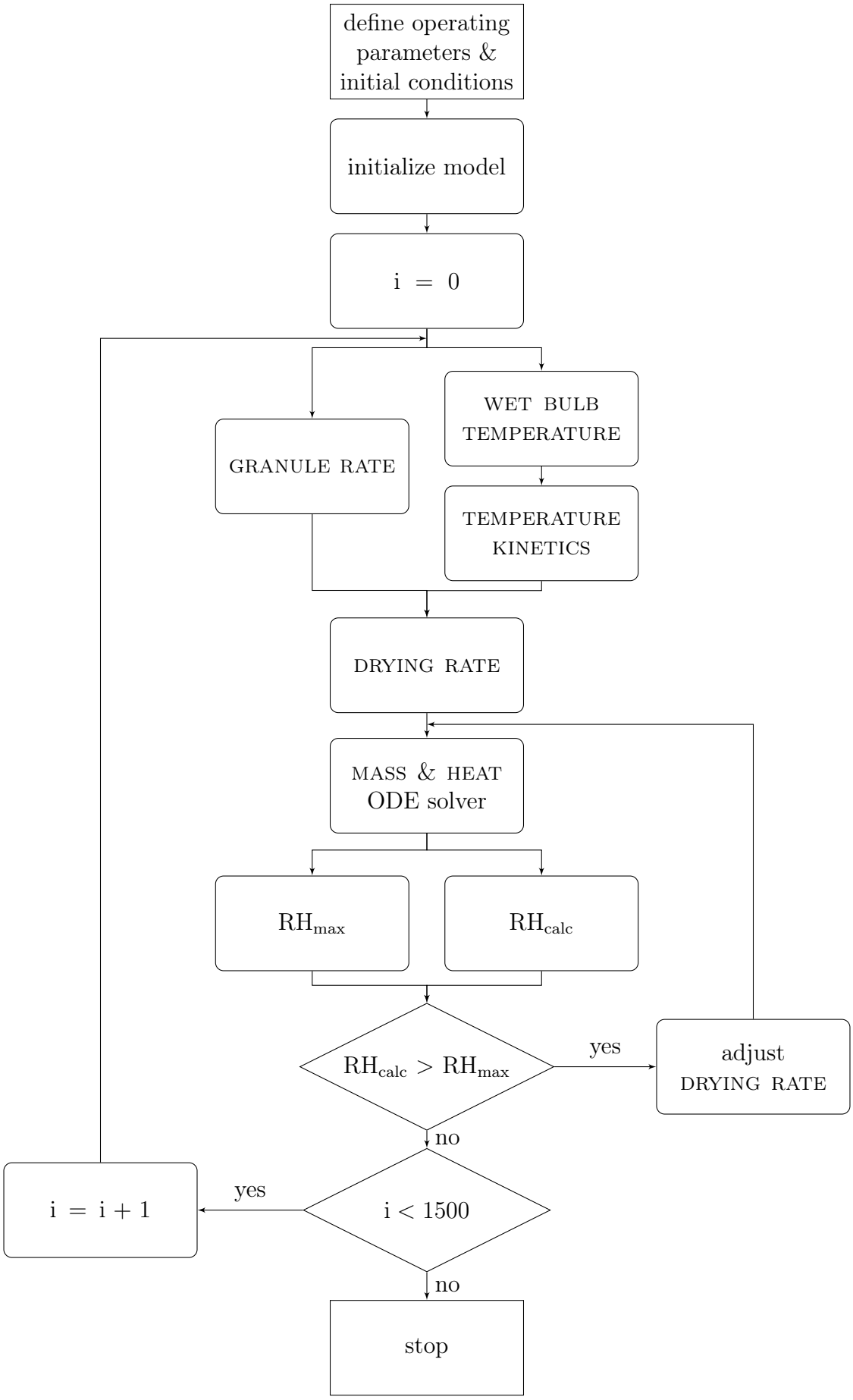

Figure 4.2: A simplified visualisation of the algorithm in the model.

5
Method and Material

In this chapter the materials and equipment used for the experimental work is presented and discussed. Further the laboratory method for determining vital properties of the granules before, during and after the drying and coating is presented.

5.1 Equipment

5.1.1 Fluidised Bed Dryer

The dryer which has been used to perform the drying experiments throughout the thesis is a fluidised bed batch dryer in pilot scale. The dryer equipment allows the operator to specify the temperature which the incoming air will be heated to and the flow rate of the air. The flow rate needs to be high enough to fluidise the solids, but not so high that the solids are pneumatically blown away from the dryer. Thus in this thesis the flow rate of the air has been investigated between $600\,\mathrm{m^3\,h^{-1}}$ to $800\,\mathrm{m^3\,h^{-1}}$. In the thesis an sensitivity analysis was performed on batch size, i.e. how the initial weight of solids which was added to the dryer influenced the drying kinetics. Just as with the flow rate of the air restrictions did apply to the maximum and minimum mass. In a typical drying in the pilot plant approximately 15 kilograms of solids are used in the dryer. It was determined that during the sensitivity analysis the mass of solids in the dryer should not exceed 22 kilograms nor subceed 9 kilograms. These limits were imposed to ensure proper fluidisation.

5.1.2 Fluidised Bed Coater

To determine how the moisture content of the granules before the coating affects the shelf life stability of the product a few coatings has been performed. The coater used in this thesis is a pilot scale fluidised bed batch coater. The process has throughout the thesis been performed at standard conditions, with the exemption of instructions given to the operators to begin the coating process immediately after fluidisation has been achieved.

5.2 Laboratory Procedures

In this section the procedures and methods used to determine the moisture content, enzyme stability and enzyme activity of the granules before, during and after the drying and or coating is presented.

5.2.1 Granule Moisture Content

In all the drying experiments small granule samples were taken from the dryer with 1 minute intervals throughout the drying. The purpose was to determine the moisture profile of the drying as a function of the drying time. Immediately after sampling the granules were put in an small, labeled and airtight container which was stored for later analysis.
To experimentally determine the moisture content of the granules a small aluminium tray was labeled and its weight to 4 decimal points of a gram was recorded as m_{tray}. Subsequently approximately 5 grams of the granule sample were added to the tray. The weight of the granules were recorded to 4 decimal points of a gram as m_{sample}. The tray and the granules were then stored in an oven at 105 °C. After a minimum of 24 hours the trays were removed from the oven and the total weight of the tray and the granules were recorded to 4 decimal points of a gram as m_{end}. Hence the fraction of moisture in the granules can be calculated according to Equation 5.1 below.

$$W_{105} = \frac{m_{sample} - (m_{end} - m_{tray})}{m_{sample}} \tag{5.1}$$

With W_{105} being the percentage of the initial sample weight which has evaporated after being stored for 24 hours at 105 °C. Finally the fraction of solid material, Solid%, can be calculated by Equation 5.2 below.

$$\text{Solid\%} = 100 - W_{105} \tag{5.2}$$

5.2.2 Enzymatic Stability

To determine the enzymatic shelf-life stability of enzyme granules in this thesis an accelerated trial was used. To determine the stability glass vials were filled with the product of interest. The vials were sealed airtight and subsequently divided into a control group which was stored in a freezer at −18 °C and a sample group, which is stored in an oven at 50 °C. The samples were then incubated in their respective environment for 2 to 3 weeks. The control vial which was stored at −18 °C was observed to exhibit only an insignificant decrease in activity at the end of the incubation due to the low temperature, and were as such essentially unaffected by the time in the storage. Meanwhile the vial which was stored at 50 °C were observed to exhibit a change of activity corresponding to months of storage at normal conditions. The enzyme activity of the two samples were then experimentally measured, see subsection 5.2.4. To obtain a relative measurement of the stability and thus allow comparison between batches, the freezer sample is used as a reference. Hence the stability is calculated from the enzyme activity per the relationship in

Equation 5.3.

$$\text{Enzyme Stability} = \frac{\text{Activity, } 50\,^{\circ}\text{C sample}}{\text{Activity, } -18\,^{\circ}\text{C control sample}} \tag{5.3}$$

Concern should be taken when reviewing results from an accelerated trial. Since the oven sample is stored at 50 °C, which likely is a higher temperature that what the product can be expected to be stored at during its life-time, question arises concerning how well the results represent the actual stability. It is not improbable that other kinetics and mechanisms may influence the enzymes when they are kept at 50 °C rather than room temperature. Hence it should be taken into consideration that the aforementioned experimental procedure only with certainty can establish the stability of the enzymes at 50 °C, not at other temperatures or humidities. However the method likely provides an acceptable indication of the relative enzyme stability.

5.2.3 Coating Yield

In addition to using the enzyme stability as a measurement of the effect of moisture in the granules on the final product, coating yield is used to measure the effect of the coating on the activity. The coating yield is calculated according to Equation 5.4.

$$\text{Coating Yield} = \frac{\text{Activity, Coated sample}}{\text{Activity, Uncoated sample}} \tag{5.4}$$

A high coating yield implies that the activity of the coated sample is comparable to the activity of the uncoated sample. Meanwhile a low coating yield implies that as a consequence of the coating, the activity of the coated sample is considerable lower than the uncoated sample.

5.2.4 Enzymatic Activity

The measurements of the enzymatic activity of samples were performed by personnel at Novozymes QC lab.

6

Experimental Results

In this chapter the results from the experimental work is presented. Actual drying curves from a batch fluidised bed dryer are shown. Deviations between theoretical and actual drying curves are discussed and motivated. The effect of vital drying parameters are discussed with data from sensitivity analyses as background. The data of enzyme stability of product granules with varying moisture contents are presented.

6.1 Drying Profiles

In this thesis a significant amount of experiments was performed to determine the properties and kinetics of the drying. During the experiments the temperature of the bed has been measured by a temperature probe. To determine the progress of the drying on the granules small samples of the solids was taken every minute and the corresponding moisture content was measured.

6.1.1 Placebo Drying

To determine the critical drying kinetics a batch of granules without enzymes, henceforth denoted as placebo granules, was performed. In Figure 6.1 below the moisture profile of placebo granules as a function of drying time in a pilot scale fluidised bed dryer is shown. The drying was performed with an incoming air temperature of 80 °C, 700 $m^3\,h^{-1}$ and with approximately 14 kg of solids. As can be seen the experimentally determined drying curve deviates from the drying curve which the theory proposes. From Figure 6.1 it is clear that a significant portion of the drying is in the constant rate period. Thus it suggests that the drying is essentially completely limited by external mass transfer, i.e. the properties of the air. It is believed that the internal mass transfers are observed to be minute due to the small particle size of granules. Hence when the surface begins to dry out the distance which the moisture inside has to diffuse is so small that its effect is insignificant. Furthermore, with the small particle size combined with the low X_{eq}, the granules are essentially dry when the surface dries out due to the high surface area to volume fraction. When considering the corresponding temperature profile additional deviations from the theory can be observed. Unmistakably the temperature initially decreases. The procedure for every experiment was to allow the dryer to pre-warm during the granulation. It is likely that whilst the granules are heated by the pre-warmed equipment as they

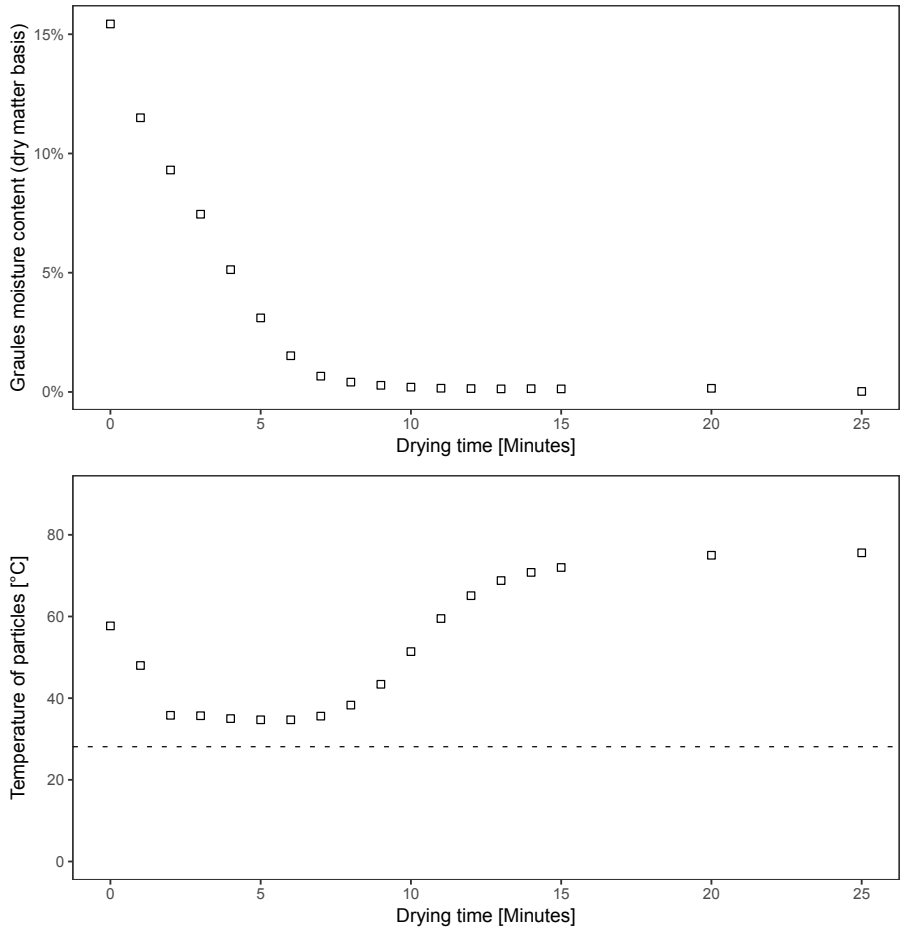

Figure 6.1: Moisture content on dry matter basis and temperature of placebo granules as a function of time in pilot scale batch drying. The dashed line in the lower subfigure is the calculated wet-bulb temperature of the incoming air. The drying was performed with an incoming air temperature of 80 °C, 700 $m^3\,h^{-1}$ and with approximately 14 kg of solids.

are added to the dryer, the temperature measured by the probe could be misleading since the probe is heated during the pre-warming. The effect is nonetheless negligible.
For all experiments the drying has consistently been performed for 40 minutes, however as observed in Figure 6.1 the drying is essentially completed after 15 minutes. Thus in future figures the x-axis will be limited, unless specified, to visualise the first 25 minutes of the drying which are the most relevant.

6.1.2 Enzyme Loading

Insofar only the kinetics of placebo granules have been considered. In order to determine the effect of enzymes on the drying kinetics additional experiments, adhering to the procedure from earlier experiments, were performed. The enzyme which has been used in the following experiments is an α–amylase. The granulation has been performed with two different loadings. The basis for the enzyme loading is determined by an arbitrarily chosen activity, a_0. In Figure 6.2 below the moisture content profile during the drying of placebo granules and α–amylase granules with activity

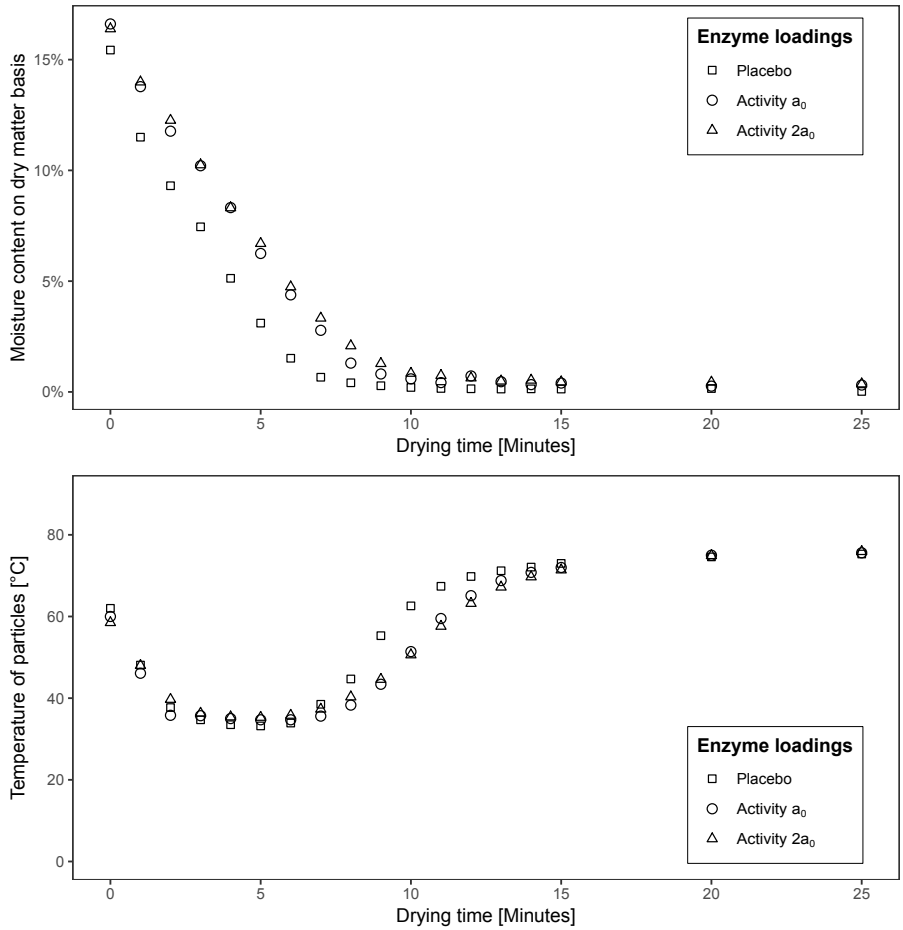

Figure 6.2: Moisture content and temperature of granules as a function of enzyme loading and time. The drying was performed with an incoming air temperature of 80 °C, 700 $m^3\,h^{-1}$ and with approximately 14 kg of solids.

a_0 and $2\times a_0$ respectively are visualised. It is observed that there is a noticeable difference between the enzyme granules and placebo granules. The placebo granules exhibit a faster drying which is to significant degree is limited by external mass transfers, i.e. occurs in the constant rate period. Meanwhile the enzyme granules are shown to dry slower during the constant rate period than the placebo counterpart. In addition the enzyme loaded granules display a larger falling rate period which can be observed to increase with increased enzyme loading.

6.1.3 Additives

The formulation for the granulated enzymes is not constant, but rather changes depending on the enzyme and the intended application of the product. In some cases additives are added to improve the characteristics such as sensitivity to surrounding environment, activity or shelf-life. These additives are of such nature that they are likely to affect the drying kinetics to a significant degree and are as such of vital importance to quantify and determine for simulation applications. Hence the effect of additives was investigated by comparing three different formulations. All the experiments were performed on placebo granules.
In figure Figure 6.3 the moisture content and temperature profile from the exper-

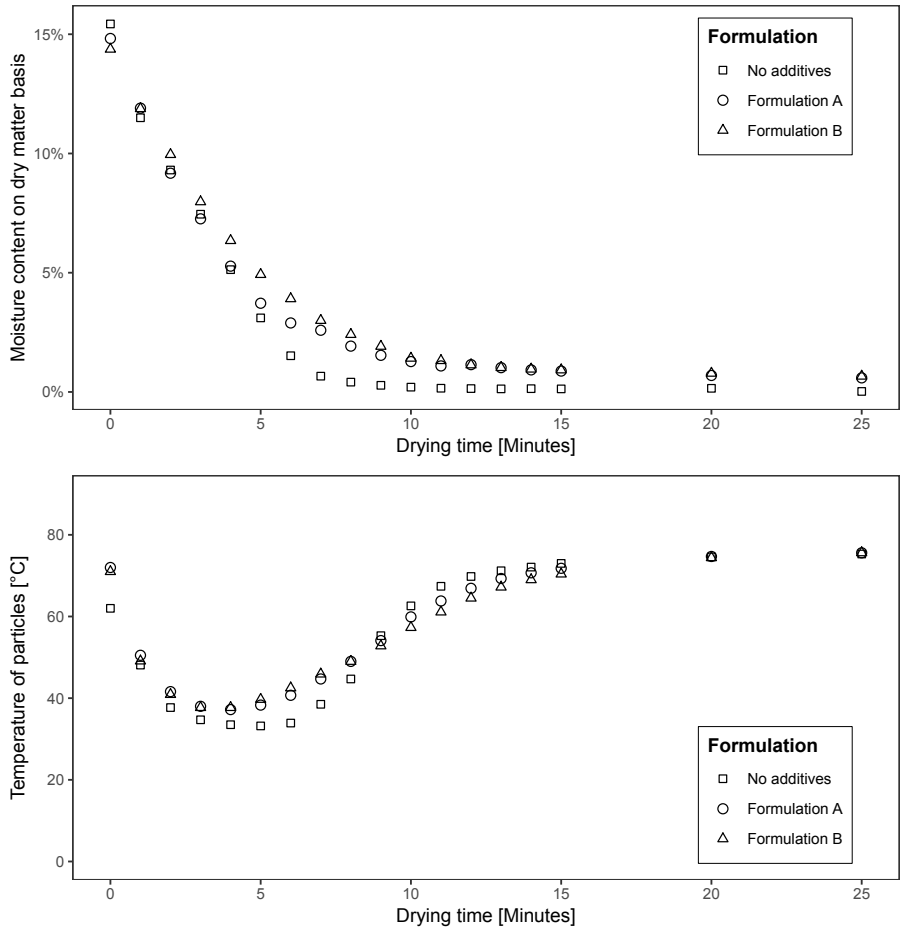

Figure 6.3: Moisture content and temperature of granules as a function of formulation and time. All formulations are placebo. The drying was performed with an incoming air temperature of 80 °C, 700 $m^3\,h^{-1}$ and with approximately 14 kg of solids.

iments with additives is shown. As is observed there are significant effect to the drying kinetics when additives are used. The 'No additives' behaves as expected, much like Figure 6.1. However when additives are used the granules exhibit altered kinetics. During the constant rate period 'Formulation A' and 'Formulation B' hold on to the water more than the samples with no additives. As such the drying takes slightly longer.

Furthermore, when the drying has progressed so far that the drying enters the falling rate period the formulations exhibits different drying kinetics. With 'No additives' the falling rate period is rather insignificant and constitutes only a small fraction of the complete drying. However for the two other formulations with additives the falling rate period is significantly more pronounced. 'Formulation B' exhibits an extremely smooth and rounded drying profile whilst 'Formulation A' is somewhere in between the other two. Finally the 'No additives' reaches a X_{eq} of about 0.047 % after 40 minutes of drying. Meanwhile 'Formulation A' and 'Formulation B' was measured at 0.545 % and 0.707 % moisture content respectively after an equal drying time. Hence the additives seem to exhibit hygroscopic properties which causes the different kinetics.

6.1.4 Sensitivity Analysis

Of the operational parameters of the dryers, i.e. flow rate and temperature of the air, humidity and mass of solids, there is some design space available – however restrictions do apply. For example, if the velocity of the air through the bed is too high there's a risk that the solids will blow away, and a too low velocity results in an insufficient fluidisation. In an equal manner a high air temperature might damage the enzymes, whilst too cold air equals an ineffective drying. Thus consideration must be observed when changing operational parameters of the dryer.
In order to determine the effect of the operational parameters of the dryer on the drying kinetics a sensitivity analysis was performed. The parameters investigated was air flow rate, air temperature and the mass of solids in the dryer. The humidity of the air is likely to significantly affect the drying, however there was no feasible method to control the humidity of the incoming air with the equipment available, hence it was not investigated. Nonetheless the humidity and temperature of the incoming air was recorded before initialising the drying.

Air Temperature

The temperature of the incoming air has a significant effect on the drying kinetics. Literature suggests that whilst the solids in the bed does not necessarily reach the wet-bulb temperature in the bed, they do approach the corresponding T_w of the incoming air. Hence the temperature of the incoming air will likely primarily affect the drying in the constant rate period at which point the drying of the solids is limited by external parameters.
The sensitivity analysis of the incoming air temperature was performed at 70 °C, 80 °C and 90 °C. In Figure 6.4 the moisture content profile for each respective temperature is visualised. It can be observed that the drying rate indeed increases with a higher temperature of the incoming air.
With an increased temperature of the incoming air the amount of water which the air can saturate increases. Hence theoretically the amount of air required to separate the moisture from the solids decreases. However as was shown earlier the air does not actually fully saturate – hence this does not necessarily have to be true. However with an increased temperature the rate of the drying increase, as was shown in Figure 6.4, thus the time, and hence the amount of air assuming fixed flow rate, decreases. Thus the process could be economically investigated to determine if the cost of increasing the temperature of the air is supported by the reclaimed expenses of heating a smaller volume of air.

Air Flow Rate

A sufficient flow rate of air is necessary not only for the bed to become fluidised but also to achieve a satisfactory mass and heat transfer in the bed. As with the air temperature it is expected that the effect of the flow rate will primarily be observed in the constant rate period, in which the rate limitation is dependent on the external properties. An increased flow rate results in that the thickness of the air-surface boundary layer is thinner. Hence the distance the evaporated moisture will be transported from the surface of the solids to the air across the film will be smaller and hence the drying rate will increase.

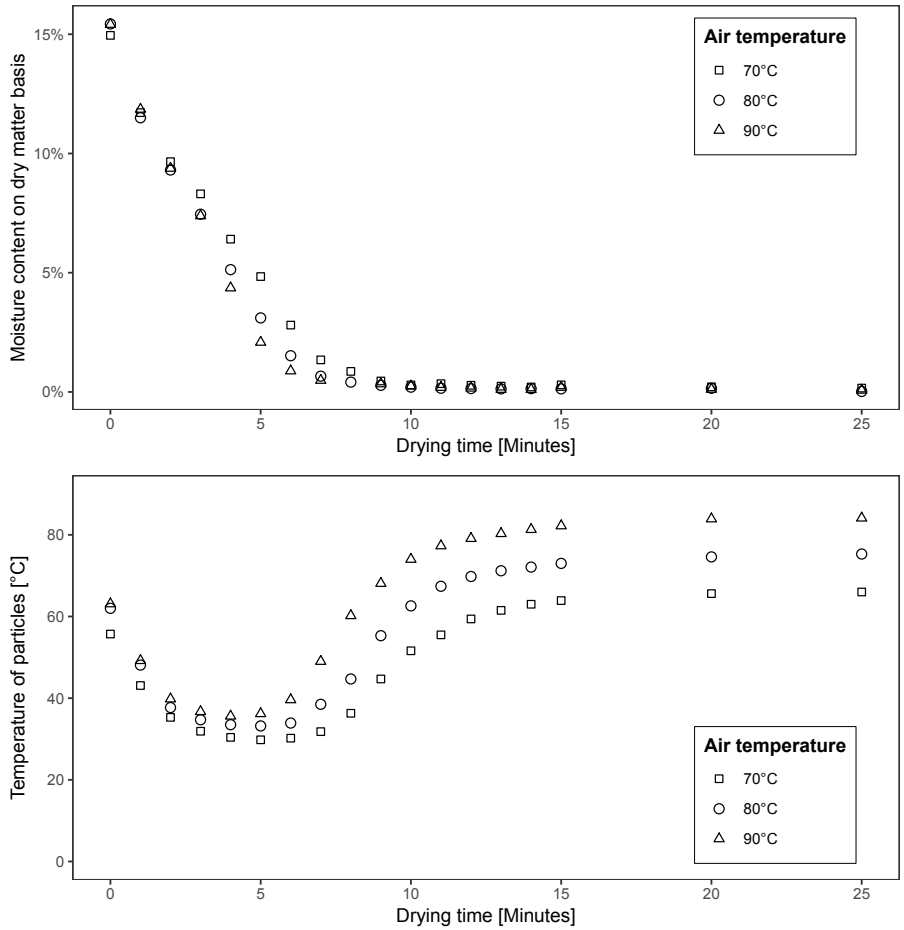

Figure 6.4: Moisture content and temperature of granules as a function of time air temperature and time. The drying was performed with a flowrate of 700 $m^3\,h^{-1}$ and approximately 14 kg of solids.

In Figure 6.5 the results from the data gathered from a sensitivity analysis of the flow rate is shown. It's observed that the drying rate decreases with a decrease in the flow rate respectively increases with a increased flow rate. In addition it is observed that whilst the drying progresses faster the temperature of the solids is independent on the flow rate. Hence this observation confirms the theory suggesting that the rate limiting kinetic during the constant rate period is the mass transfer of moisture across the air-surface interface.
The rate of drying during the constant rate period in Figure 6.5 shows a significant correlation to the flow rate, displayed in Figure 6.6.

Mass solids

The mass of solids added to the dryer is likely to effect several of the important mass and heat transfer phenomena in the bed, and hence also effect the drying kinetics. As the mass of solids increase the flow rate of the air required to achieve fluidisation will also increase. If the mass of the solids is drastically decreased the flow rate will be required to be smaller to compensate for the greater chance of pneumatic transport.
To investigate the effect of the mass loaded to the dryer a sensitivity analysis was

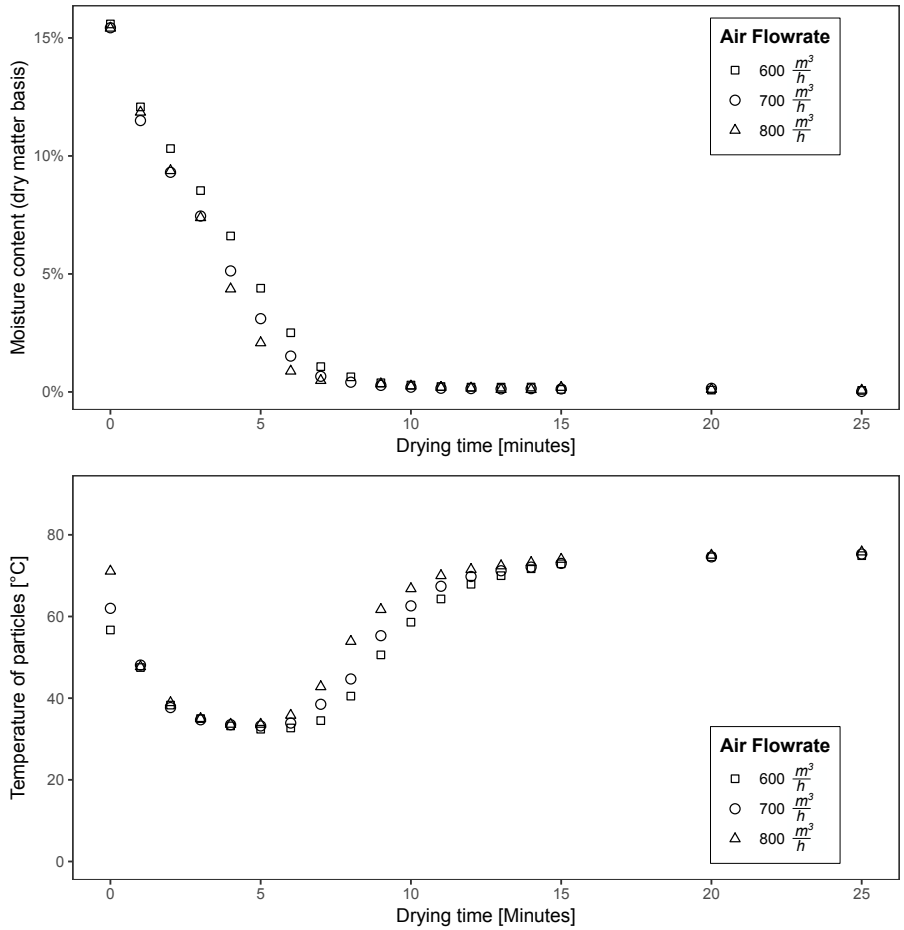

Figure 6.5: Moisture content and temperature of granules as a function of air flow rate and time. The drying was performed with an incoming air temperature of 80 °C and approximately 14 kg of solids.

performed by loading the dryer with 9.37 kg, 12 kg and 21.7 kg of granules. The moisture content profile and temperature of solids gathered during these experiments are presented in Figure 6.7. As is observed – assuming a fixed flow rate of air – a small batch of solids dries quicker than a larger batch.
This conclusion is trivial since with an increased mass of solids loaded to the dryer, an equal fraction of moisture is added. Thus the quantity of moisture required to be removed from the solids increase and hence the time required in the dryer increases.

6.2 Enzyme Stability

The stability tests were performed on both coated and uncoated enzyme granules. The reasoning was that obtaining the data of the stability of the enzymes in the raw granules and the coated granules would provide a further insight in any possible deactivation. Hence if a correlation between the stability and the moisture of the raw granules, determining the stability of both the coated and uncoated can provide additional understanding of the deactivation mechanisms.
Granulation and drying experiments to produce material for the stability tests was performed two weeks after initiating the project. To obtain satisfactory data of

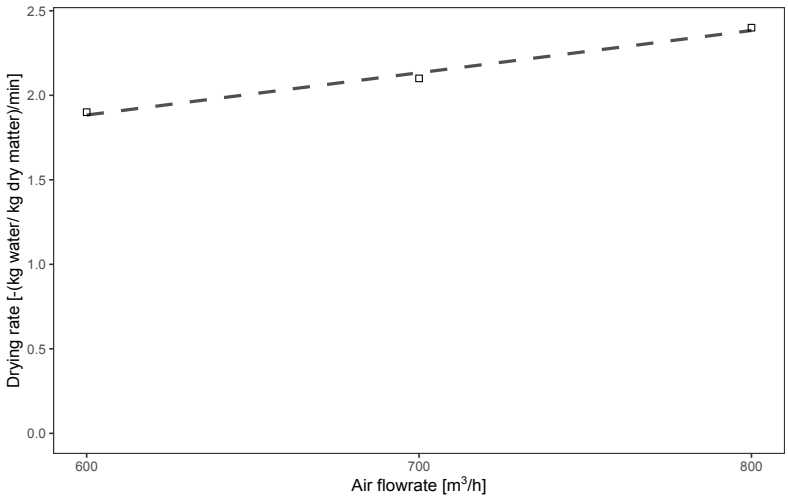

Figure 6.6: The rate of drying as a function of air flow rate. Dashed line is the trend line showing the linear correlation.

the stability a distribution of moisture in the samples was desired. The designed procedure was to obtain four samples with a moisture content of 8 %, 4 %, 2 % and 1 % respectively. However, since when the experiment was performed no data of the drying profile of the granules was available, it proved difficult to estimate how dry the granules were. The resulting samples from the first experiment was determined to have a moisture content of 0.59 %, 0.72 %, 0.40 % and 0.28 %. The corresponding measured stability of the coated samples were as expected all unsatisfactorily since the produced samples had a poor distribution and all had a very low moisture content. The measured residual enzyme activity of the coated samples are shown in Figure 6.8. In essence there is no distinguishable difference of stability between the samples. The deviations in Figure 6.8 can likely be attributed to the confidence level of the measuring method.
Hence a new iteration of the stability experiments was performed. This attempt used 3 samples rather than 4 to minimise unnecessary workload on laboratory facilities. Again a moisture distribution of the samples corresponding to approximately 8 %, 3 % and 1 % was desired. The produced samples were determined to have a moisture content of 7.88 %, 1.66 % and 0.80 %. Each of the samples was divided into two fractions, one for coating and the other as a reference of the uncoated granules.
In Figure 6.9 the stability values for the coated granules from the second iteration of the stability tests are shown. It can be observed that the two samples with a low moisture content (1.66 % and 0.80 %) exhibit a residual activity resembling those from the first iteration (which had a moisture content of 0.59 %, 0.72 %, 0.40 % and 0.28 %), shown in Figure 6.8. However the sample with a moisture content of 7.88 % does display a significant decreased enzyme stability.
Whilst the residual activity provides a relative measure of the enzyme shelf-life the actual enzyme activity in itself also has to be considered. While a product might exhibit an excellent stability it is not a feasible product if its actual absolute activity is low. In Figure 6.10 the coating yield (see subsection 5.2.3), raw granule stability and coated granule stability from the second iteration of the stability test are shown. The activities have been normalised to the highest value in the data set – raw granule at 0.80 % moisture content. It is observed that the 7.88 % sample

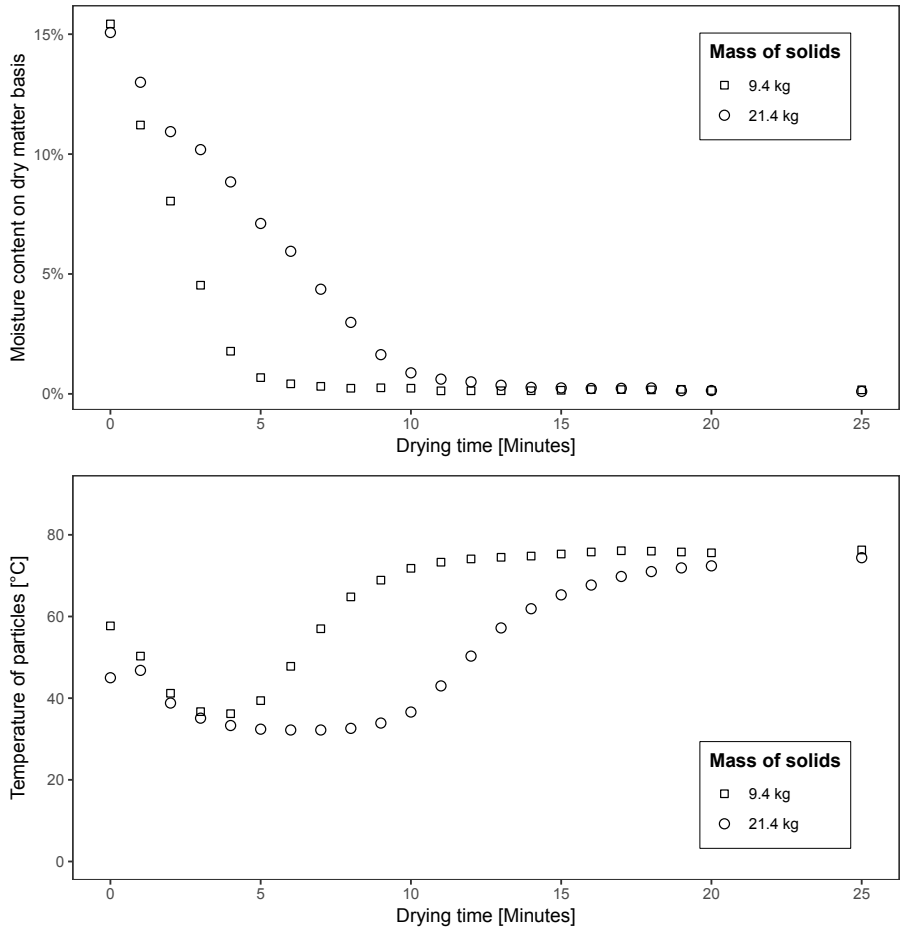

Figure 6.7: Moisture content and temperature of granules as a function of mass of solids and temperature.

exhibit a slightly worsened residual activity of both coated and uncoated samples in comparison to the 1.66 % and 0.80 % samples. However the 7.88 % was shown to exhibit an extremely low coating yield in comparison to the other samples. The coating yield is a measurement which signifies the difference in absolute activity between the coated and the uncoated sample. Hence Figure 6.10 shows that whilst the stability of the uncoated and coated samples are essentially the same, the activity of the coated sample is substantially lower.
As such the granules with a moisture content of 7.88 % not only exhibit a decreased residual stability for both the coated and uncoated samples but also a significantly lower coating yield. The latter suggests that the enzymes in the coated samples have been damaged during the coating process.

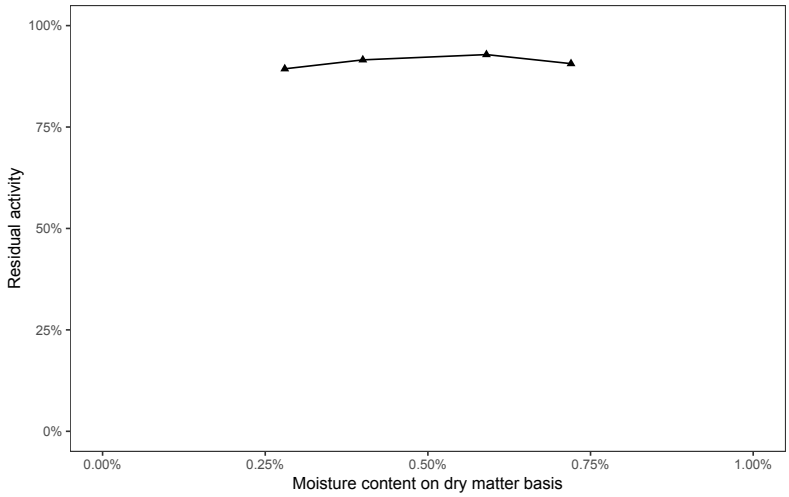

Figure 6.8: Residual activity of coated samples from the first iteration of the stability trials as a function of moisture content.

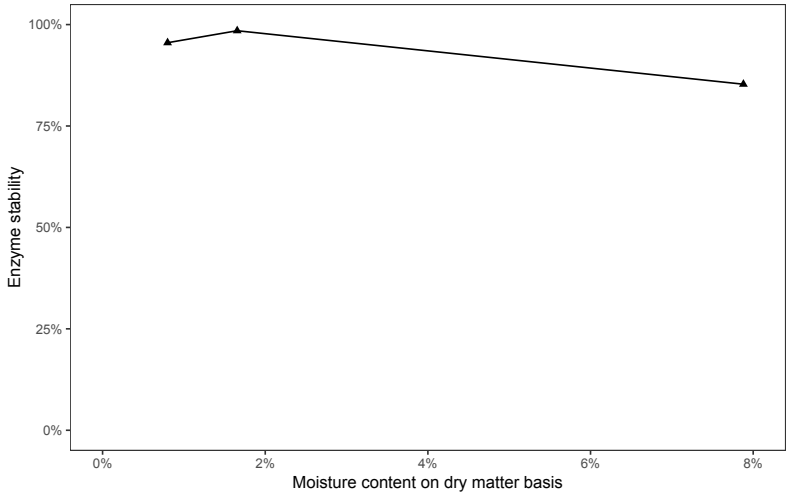

Figure 6.9: Residual activity of coated samples from the second iteration of stability trials as a function of moisture content. The samples were incubated for 2 weeks.

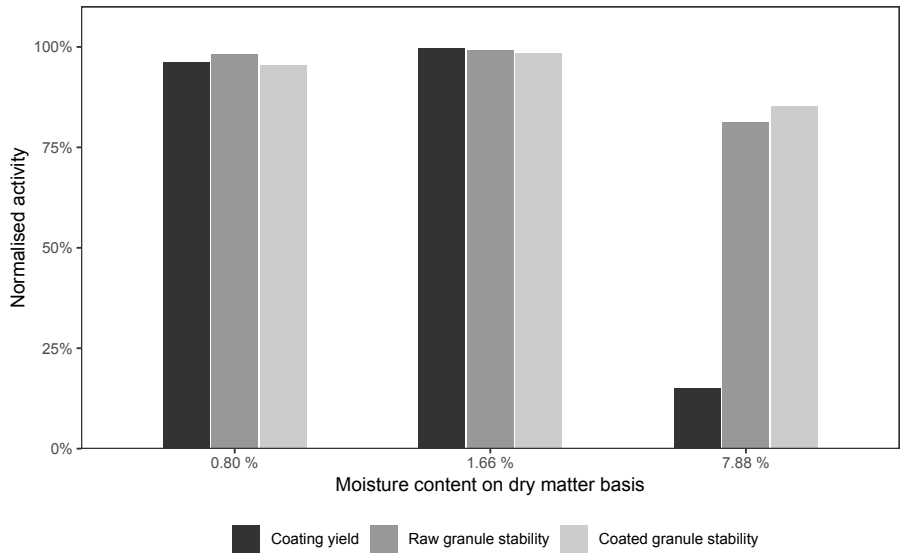

Figure 6.10: Coating yield, raw granule stability and coated granule stability of samples from the second iteration. The samples were incubated for 2 weeks.

7
Simulation Results

In this chapter the results from the developed mathematical model is presented and compared to the experimental data from chapter 6. The purpose is to compare how well the developed model describes a fluidised bed batch dryer. A parameter sensitivity analysis is performed to investigate how well the model can predict changes of operating parameters such as temperature, air flow rate, formulation, batch size and enzyme loading.

7.1 Placebo

In Figure 7.1 the results from simulating a typical drying of placebo granules without additives at standard conditions is shown. The experimental data presented in Figure 7.1 is the same as in Figure 6.1. The mass of solids is specified at 14 kg, the temperature at 80 °C and the flowrate at $700\,m^3\,h^{-1}$.
As can be observed in Figure 7.1 the model simulates the moisture content progress acceptably accurate. However the simulated temperature curve deviates significantly from the experimentally determined data. Initially the simulation decreases in temperature rapidly whilst with the experimental data a slower decrease of the temperature can be observed. This is likely due to the latent heat which the equipment obtain whilst pre-heating, before the granules are added to the dryer. The heat absorbed by the equipment cause a retardation of the initial temperature dive. Since the model does not account for heat transfer with the equipment the model is not able to account for this effect. However the model does to some extent reasonably simulate the temperature in the constant rate period. Finally, the simulated temperature at the end of the drying is higher than the corresponding temperature determined experimentally. These properties and weaknesses will be further discussed in chapter 8.
With consideration to the discussion above the temperature will not be considered in further figures.

7.2 Enzyme Loading

It goes without saying that a vital property which the model ought to take into account is the loading of enzymes. From prior experimental data in chapter 6 it was shown that the addition of enzymes cause a significant effect on the drying kinetics

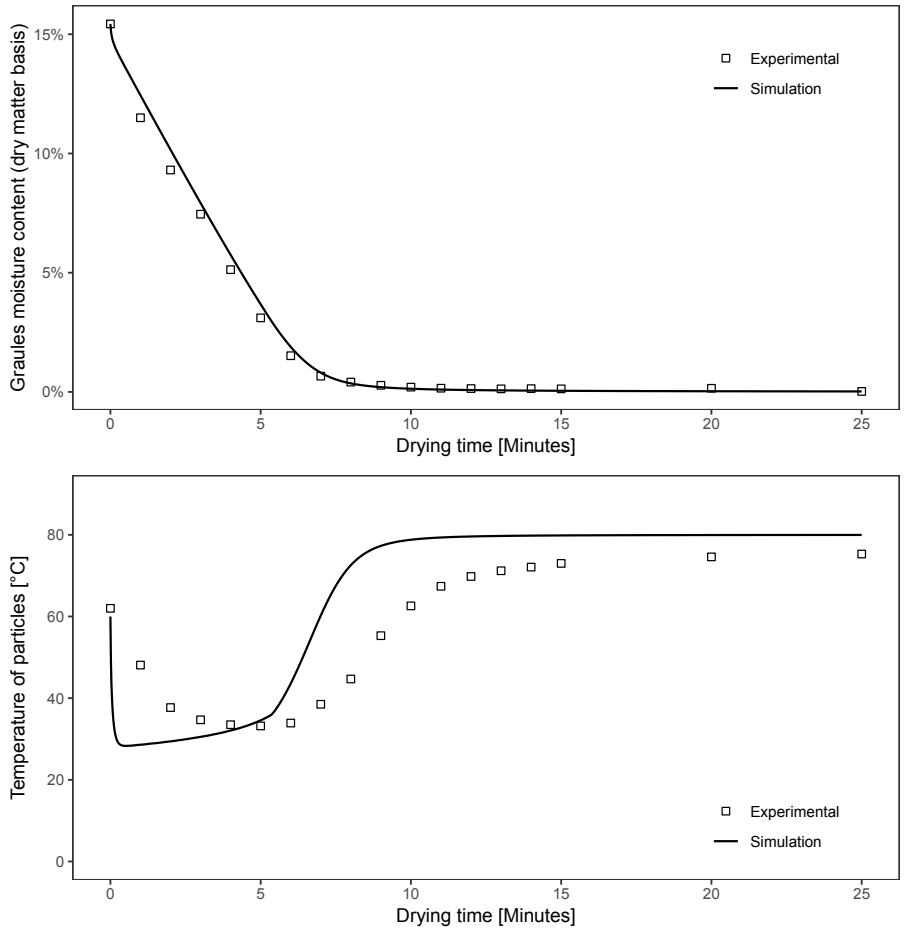

Figure 7.1: Moisture content and temperature profiles of experimental data (points) and simulation (lines) as a function of time. The experimental drying was performed with an incoming air temperature of 80 °C, 700 $m^3\,h^{-1}$ and with approximately 14 kg of solids.

and a clear correlation between the activity and the drying rate was shown. Further, the addition of enzymes was shown to alter the X_{eq}, causing the granules to contain more moisture at the end of the drying.
In Figure 7.2 the experimental data is compared to the simulations. The operating parameters in the model was specified to: 80 °C, 700 $m^3\,h^{-1}$. The mass of the solids was specified at 14.0 kg. From the figure it can be observed that be model predicts the drying of granules with different loading of enzyme with only slight deviations from the experimental data.

7.3 Sensitivity Analysis

It is required and expected that the model is able to account for changes of the operating parameters of the dryer. In chapter 6 the effect of vital operating parameters on the drying kinetics was experimentally determined. These data sets are now used to investigate how well the developed model describes the dryer.

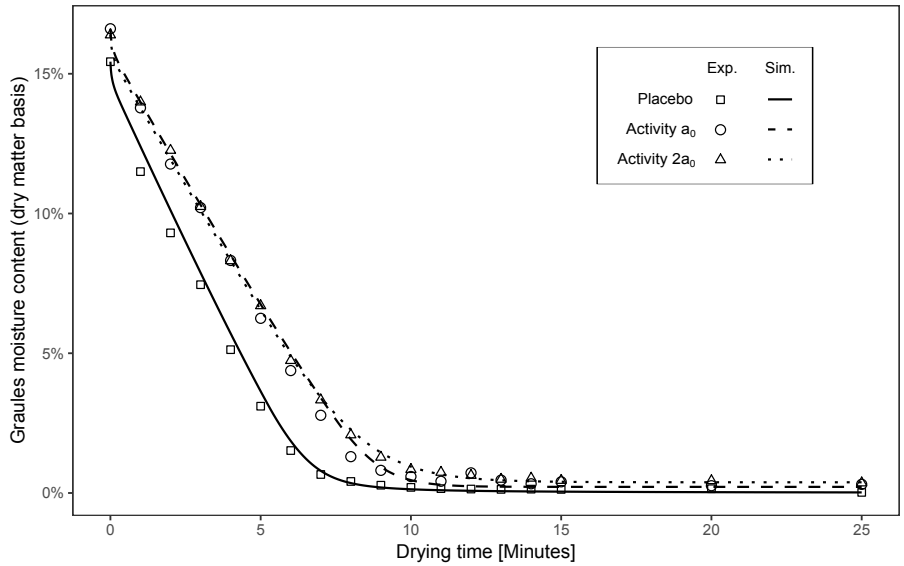

Figure 7.2: Moisture content profiles of experimental data (points) and simulation (lines) as a function of time and enzyme loading. The experimental drying was performed with an incoming air temperature of 80 °C, 700 $m^3\,h^{-1}$ and with approximately 14 kg of solids.

Temperature

By changing the temperature of the incoming air in the model comparisons can be made of how well the model accounts for a change of said operating parameter. In the mathematical model the temperature and humidity of the incoming air and the drying rate in the prior unit step determines the wet-bulb temperature, T_w, see section 4.2. Hence the temperature of the incoming air will both influence the rate of the drying during the constant rate period but also the water-carrying capacity of the outgoing air.
In Figure 7.3 a sensitivity analysis of the incoming temperature in the model was performed. The simulated results, lines, are compared to the experimental data, points.

Flow rate

In Figure 6.5 it was shown that with an increased flow rate of the air the drying rate increases. Hence to validate the model it is of interest to investigate how well the simulations accounts for a change of said parameter. As in subsubsection 6.1.4 and Figure 6.5 the flow rates which are investigated are 600 $m^3\,h^{-1}$, 700 $m^3\,h^{-1}$ and 800 $m^3\,h^{-1}$.
The results from the simulations are presented in Figure 7.4 and are compared to the experimental data. As is observed in the figure the model satisfactory predicts the effect of changes in air flow rate.

Batch size

In Figure 6.7 the effect of batch size was investigated experimentally. Drying of a batch which was made as large as the equipment allowed weighed in at 21.4 kg

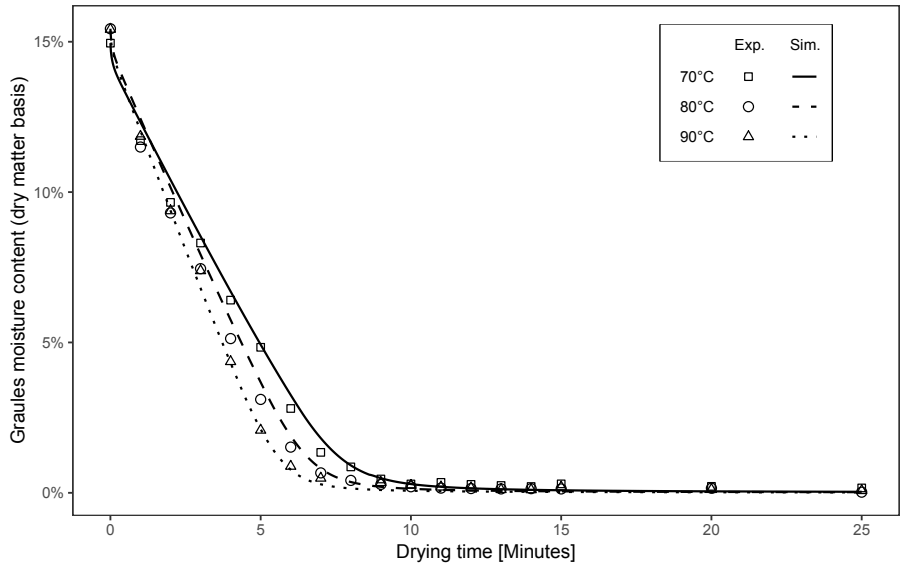

Figure 7.3: Comparison of experimental data (points) to the simulation (lines) at different temperatures of the incoming air. The experimental drying was performed with an incoming air flow rate of $700\,\mathrm{m^3\,h^{-1}}$ and with approximately 14 kg of solids.

and one as small as possible, measured at 9.4 kg, was performed. It was shown, as expected, that the batch size to a large extent influence the systems drying kinetics. In Figure 7.5 the results from the simulations of different batch sizes are presented. The temperature was specified at 80 °C and the flowrate at $700\,\mathrm{m^3\,h^{-1}}$. The mass of the solids was specified at 9.4 kg and 21.4 kg respectively.

Formulation

In chapter 6 it was shown that the additives used in different formulations cause a significant effect on the drying kinetics. In Figure 6.3 it was observed that both 'Formulation A' and 'Formulation B' resulted in a higher X_{eq} than the 'No additives' and a significantly higher X_{cr}. Hence it is vital that the model is able to account for the additives used in the formulation.
In Figure 7.6 the results from the simulation is compared to the experimental data. As is shown the model is satisfactory capable of accounting for the additives used in the formulation. The simulation was performed at standard conditions: 80 °C, $700\,\mathrm{m^3\,h^{-1}}$ and 14 kg.

7.4 Enzyme and additives

In the simulations above the model has been compared to experimental data on how well it describes, among other things, the addition of enzymes and additives on the drying. However no simulations of enzyme and additives together has yet been performed. In this section the two are combined and the results evaluated.
In Figure 7.7 experimental data of drying α–amylase loaded granules with 'Formulation A' and with an activity of $2\times a_0$ is compared to the results from the simulation. The simulation was performed at standard conditions: 80 °C, $700\,\mathrm{m^3\,h^{-1}}$ and 14 kg.

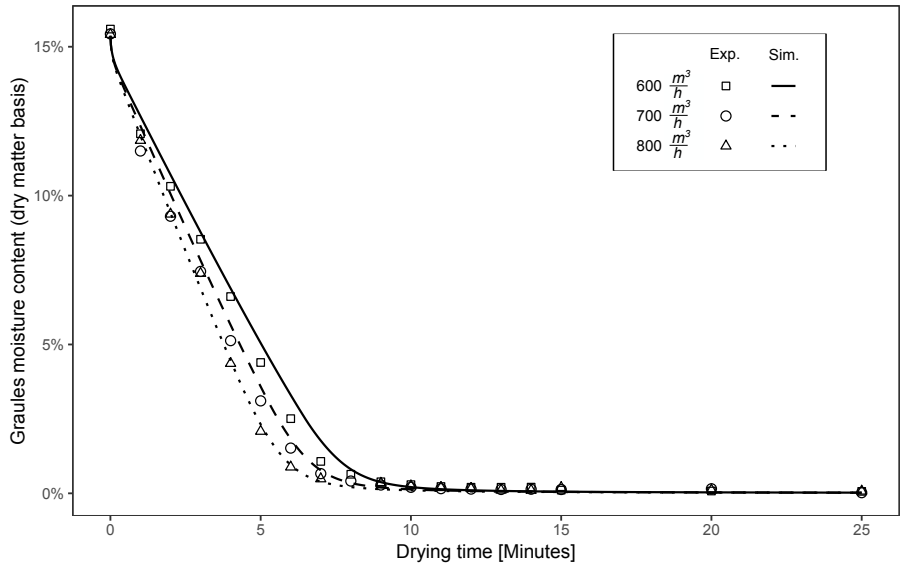

Figure 7.4: Comparison of experimental data (points) to the simulation (lines) at different flow rates of air. The experimental drying was performed with an incoming air temperature of 80 °C and with approximately 14 kg of solids.

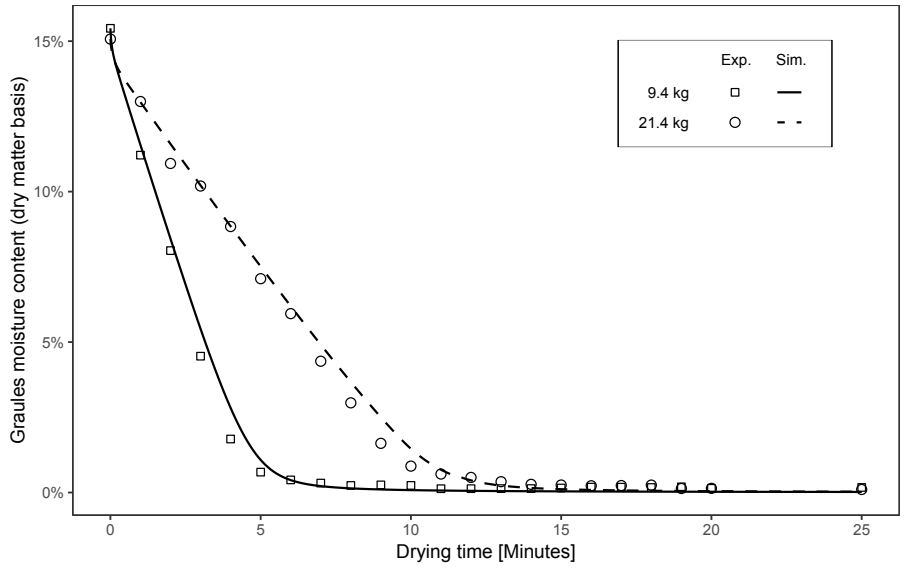

Figure 7.5: Comparison of experimental data (points) to the simulation (lines) at different batch sizes. The experimental drying was performed with an incoming air temperature of 80 °C and 700 $m^3\,h^{-1}$

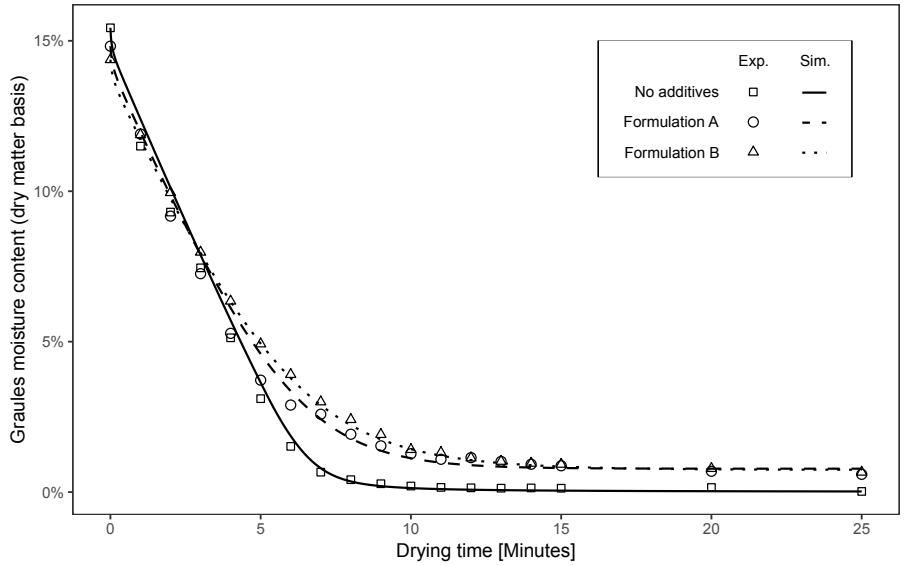

Figure 7.6: Moisture content profile of experimental data (points) and simulation (lines) as a function of time and formulation. The experimental drying was performed with an incoming air temperature of 80 °C, 700 $m^3\,h^{-1}$ and with approximately 14 kg of solids.

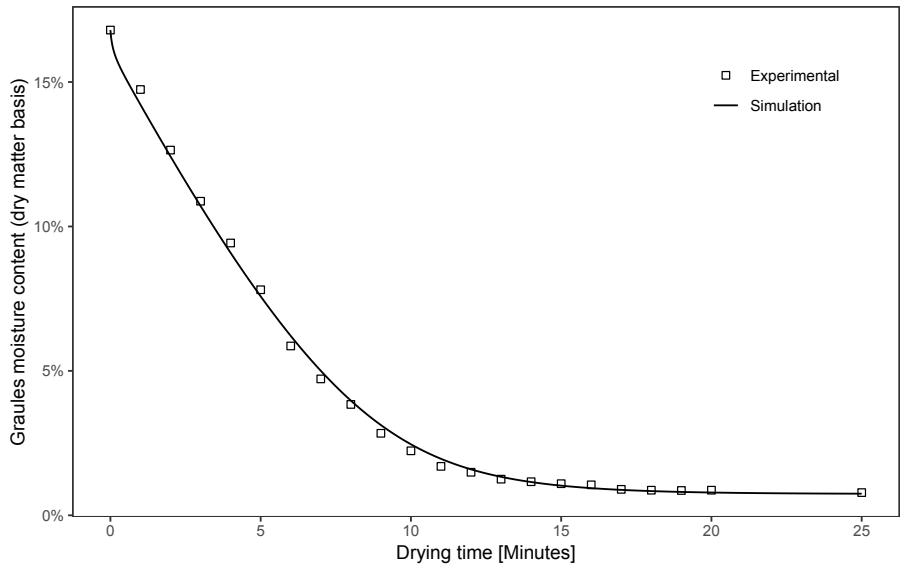

Figure 7.7: Moisture content profile of drying enzyme granules with 'Formulation B' from experimental data (points) and simulation (line) as a function of time. The experimental drying was performed with an incoming air temperature of 80 °C, 700 $m^3\,h^{-1}$ and with approximately 14 kg of solids.

8

Discussion

In this chapter the experimental results from chapter 6 and the results from the simulations in chapter 7 are discussed. First the data from the experiments from the pilot scale fluidised batch dryer is reviewed. Then the simulation results from the developed mathematical model is compared to experimental data and the model is evaluated and reviewed. Finally the results of the enzyme activity and stability at different moisture contents are considered and evaluated.

8.1 Experimental

From the performed experiments and the data gathered it was observed that the experimental drying in a batch fluidised dryer did deviate from the theoretical in several ways.
Neither the temperature of the bed nor the outgoing air reached the corresponding wet-bulb temperature, T_w, of the incoming air, see Figure 6.1. Whilst the temperature of the bed and the air was observed to decrease significantly the first minutes of the drying, the lowest measured temperature nevertheless was approximately 10 °C to 20 °C higher than the corresponding wet-bulb temperature of the incoming air. When the water activity of the raw granules just after the granulation was measured it was observed that it does not reach 100 % – hence confirming that it is not feasible for the air to become fully saturated. Hence it could be argued that constant rate period is not limited by the external mass transfer properties but that the drying rate is instead limited by internal mass transfer kinetics. In other words the constant rate period observed in the drying curves is actually the first falling rate period.
The theory suggests that the drying is to have a distinct falling rate period in which the internal mass transfer of moisture is the rate limiting kinetic. However from the data gathered in the experiments it was observed that the falling rate period was negligible. The reason might be that when the surface of the granules begins to dry out the drying has progressed to such an extent that the granule might be considered to already be completely dry. Since the granules do have a very small diameter the distance which the moisture must travel inside the granules is so small that the effect is insignificant. Essentially the granules are already completely dry when the surface begins to dry out due to the small volume to surface ratio of small spheres. Hence it is believed that the effect of the falling rate period is more prominent when drying granules with a larger diameter and thus a larger distance for the moisture to travel inside the granules.

In all experiments it was observed that the temperature of the bed initially decreases in temperature. According to the literature the temperature of the bed can initially either increase or decrease, depending on the initial temperature of the bed and the properties of the air. However caution should be observed when evaluating this behaviour. The procedure during the experiments was that while the granulation was performed the batch dryer was run empty to heat up the equipment. The probe which measures the temperature of the bed is positioned in a metal sheath suspended in the middle of the dryer. Hence when the dryer is running empty the probe and sheath heats up and retains some of that heat even after the solids has been added. Thus it is possible that the measured temperature is not a completely accurate representation of the actual temperature of the granules. In an equal manner it is likely that the steel walls of the dryer equipment heat up during the heat-up period. Hence the granules obtain some heat when they are added to the dryer. As a consequence it is deemed likely that the heated equipment might partially account for the sluggish decrease in temperature observed in Figure 7.3

8.1.1 Enzymes and Additives

In Figure 6.2 it was shown that the placebo granules do dry faster than the granules with enzymes. The effect of the enzymes increases with an increased activity. However it was shown that the X_{eq} of the samples after 40 minutes did not deviate to a significant degree. Hence the enzymes are likely to alter the drying kinetics by exhibiting a hygroscopic effect. It is likely that the enzymes bind to some of the moisture, however the strength of the binding is not very strong, and thus the moisture can evaporate from the enzyme at low temperatures.
When the formulation of placebo granules was changed to use additives a significant effect on the drying kinetics was observed, see Figure 6.3. The additives which are used in 'Formulation A' and 'Formulation B' are known to exhibit hygroscopic properties. One of the additives is a hydrate and hence has one or several water molecules bound to the salt. Some of these are known to evaporate from the salt at relatively low temperatures. Hence these properties might explain why the drying takes a longer time for 'Formulation A' and 'Formulation B' – as the temperature of the solids increases more and more of the hydrates can evaporate from the salt. However the temperature at which some of the hydrates evaporate from the salt is higher than the temperature the solids can expected to reach during a typical drying. Thus a fraction of the original hydrates will remain even after 40 minutes of drying at 80 °C. Hence this explains why after a completed standard drying cycle 'Formulation A' and 'Formulation B' was measured to have a moisture content of 0.545 % and 0.707 % respectively whilst 'No additives' was measured at 0.047 %.

8.2 Simulation

In chapter 7 the results from the mathematical model was compared to the experimentally gathered data. In this section the validity of the model and results from simulations are further discussed.
Overall the model simulates the drying satisfactory. The model is able to take vital operating parameters, such as temperature, flow rate, enzyme loading, formulation and batch size into account. In chapter 7 the model was compared experimental data

from chapter 6 and was shown to acceptably predict the changes of all operating parameters.
However the model lacks in some aspects. As was discussed in chapter 7 and observed in Figure 7.1 the model is not satisfactory capable of simulating the temperature profile of the dryer. The reason is that the model does not take heat transfer to the surrounding equipment into account. Rather the system is described as "semi-adiabatic", hence only considering heat and mass for incoming and leaving air. In addition the model does not accurately simulate the temperature at the end of the drying. From experimental data it is known that even after 40 minutes of drying at 80 °C the temperature of the bed was measured at 76 °C. Meanwhile the model predicts the bed to reach 80 °C after as little as 10 minutes. This is likely due to that the model does not take heat transfers such as radiation and conduction to surrounding environments into account. As the size of dryers increase the ratio of the volume of solids to the surface contact area of the equipment will increase (i.e. the volume of solids increase more than the surface area). Hence in larger scale operations the prior observed phenomena will likely decrease substantially.
The extent of which the incorrect temperature influence the final results is likely significant. It is possible that whilst the incorrect temperature results in incorrect drying rates, the effect is accounted for by the parameter fittings which essentially cancels out the aftermath of the deviated temperature. Using parameters to account for incorrect kinetics derived from upstream issues is not ideal, but given the time-restriction it was deemed appropriate.
Attempts were made to account for the effect of the heat transfer to the surrounding equipment. The results of these efforts are shown in Figure 8.1. As can be seen in the figure the simulated temperature profile resembles the experimental data significantly more than Figure 6.1. However this improvement is with a trade-off: the simulated data instead deviates more from the experimental data than the earlier iteration.
In the thesis there has not been any investigation into continuous fluidised bed dryers. However, since the solids in a continuous fluidised bed dryer continuously travel along the length axis of the bed it can be considered as a series of batch FBD's with a fixed residence time in each. Hence it is feasible to approximate a continuous FBD by defining a finite amount of theoretical stages in a compartment model method.

8.3 Enzyme Activity

All the four samples from the first iteration of the stability trials had extremely low moisture content and poor distribution (0.59 %, 0.72 %, 0.40 % and 0.28 %). Hence the results from these trials were of insignificant value. As was expected essentially no difference in residual activity could be observed between the samples. However one takeaway from the experiments was that the enzymes are not sensitive to high temperatures as long as they are dry. The first sample which had a moisture content of 0.59 % was taken when the temperature of the bed was 51 °C However the last sample from the same experiment, which had a moisture content of 0.28 % was removed from the bed when the temperature was measured to be 76 °C. Hence the results do show that given that the raw granules are dry they can be subjected to high temperatures for extended periods of time without significant risks to the

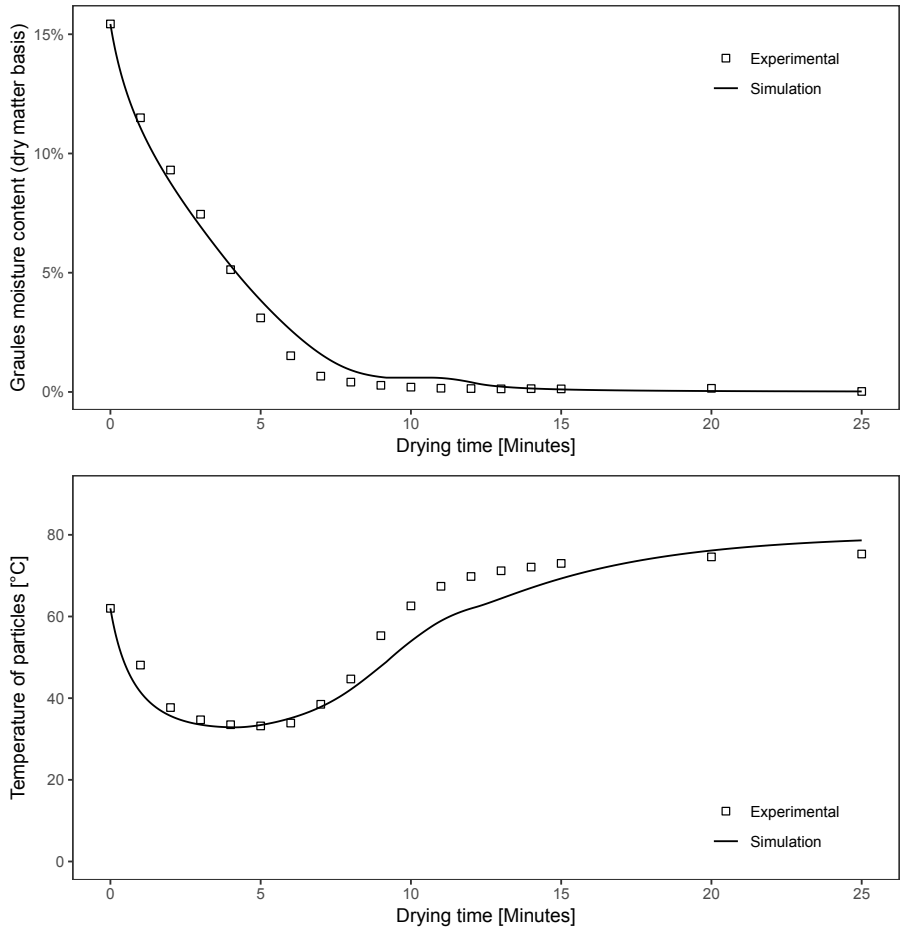

Figure 8.1: Moisture content and temperature profiles of experimental data (points) and improved simulation (lines) as a function of time. The experimental drying was performed with an incoming air temperature of 80 °C, 700 $m^3 h^{-1}$ and with approximately 14 kg of solids.

enzymes.
Due to the poor distribution of moisture in the samples in the first iteration a second experiment of the stability was performed. As was determined earlier the sample with a moisture content of 7.88 % exhibited a significant decreased stability and absolute activity. The large decrease in absolute activity was present in both the sample which had been stored at −18 °C and at 50 °C. Hence it is likely that the enzymes lose their activity whilst being coated.
When the granules are being coated in the fluidised bed coater the air temperature and humidity is continuously measured and adjusted. The temperature is typically in the range between 50 °C and 80 °C. When the granules are added to the fluidised bed coater they are quickly heated to the operating temperature of between 50 °C and 80 °C. Hence with the combined effect of the encapsulated moisture in the high moisture content samples and the high temperature the enzymes can denatured or change shape so that the activity decreases. Meanwhile the samples with a low moisture content does not exhibit the lubricant effect of the moisture, and hence does not exhibit the same inactivation of the enzymes. This might be an explanation to why the sample with a moisture content of 7.88 % can be observed to have such a significantly decreased absolute activity when coated, whilst the samples with 1.66 %

and 0.80 % does not.
As such the hypothesis suggesting that it is the moisture which is added to the granules during the coating process which is responsible for decreased residual activity is not supported. Rather the data indicates that it is the amount of moisture the granules contain when they are coated which correlates to the stability. The reason being that as they are coated the moisture is encapsulated inside. When the granules increase in temperature in the fluidised bed coater the high moisture content – acting as a lubricant – combined with the high temperature – hence increases the rate of movements – causes the enzymes to denature and thus lose its activity. The uncoated samples do not exhibit the same behaviour since the moisture is not encapsulated inside. Thus the moisture in the granules will continuously evaporate and hence keep the granules at a lower temperature than the incoming air – removing the factor which allowed the increased movements of the enzyme.

9
Conclusion

The primary objective of this thesis was to determine if any correlation between moisture content from the FBD and product shelf-life stability could be determined. From the experimental results in chapter 6 it was shown that the residual activity was lower for granules with moisture content of 7.88 % than for granules with 0.8 % and 1.66 %.
In addition it was shown that the coating yield of the high moisture content sample was significantly lower than the two samples with less moisture content. It was shown that the coating yield of the high moisture sample was approximately one tenth of the coating yield of the lower moisture samples. Hence it is likely that as the granules with a high moisture content are coated the moisture is encapsulated inside, and can act as an lubricant for the protein chains. With the combined high temperature in the coater and the lubricant effect of the moisture the enzymes can denature and hence lose activity. Consequently whilst the hypothesis behind the primary objective to some extent was correct, the most important takeaway was the substantial loss of enzyme activity during the coating of granules with high moisture content.
The developed model was in chapter 7 shown to be able to predict and simulate the moisture content profile well compared to experimental data. A sensitivity analysis of vital operating parameters such as temperature, air flow rate, batch size, enzyme loading and formulation was performed to determine how well the model is able to take them into account. However the model lack in that regard that it does not simulate the temperature of the bed good compared to the experimental data. The model does not take heat transfer to the equipment and surrounding environment into account, which likely is the cause behind this flaw.

Bibliography

[1] S. T. F. Mortier, T. D. Beer, K. V. Gernaey, J. P. Remon, C. Vervaet, and I. Nopens, "Mechanistic modelling of fluidized bed drying processes of wet porous granules: A review," *European Journal of Pharmaceutics and Biopharmaceutics*, vol. 79, no. 2, pp. 205 – 225, 2011.

[2] B. S. Yildiz, "18 - water and wastewater treatment: biological processes," in *Metropolitan Sustainability* (F. Zeman, ed.), Woodhead Publishing Series in Energy, pp. 406 – 428, Woodhead Publishing, 2012.

[3] D. Kunii and O. Levenspiel, "Chapter 2 - industrial applications of fluidized beds," in *Fluidization Engineering (Second Edition)* (D. Kunii and O. Levenspiel, eds.), pp. 15 – 59, Boston: Butterworth-Heinemann, second edition ed., 1991.

[4] S. Biran, *Stability of Enzymes in Granular Enzyme Products for Laundry Detergents*. PhD thesis, 2010.

[5] G. I. Tardos, "Wet-granulation research with application to scale-up," *China Particuology*, vol. 3, no. 3, pp. 191 – 195, 2005.

[6] S. Shanmugam, "Granulation techniques and technologies: recent progresses," *Bioimpacts*, vol. 5, no. 1, pp. 55–63, 2015.

[7] A. Kumar, J. Vercruysse, G. Bellandi, K. V. Gernaey, C. Vervaet, J. P. Remon, T. D. Beer, and I. Nopens, "Experimental investigation of granule size and shape dynamics in twin-screw granulation," *International Journal of Pharmaceutics*, vol. 475, no. 1, pp. 485 – 495, 2014.

[8] C. J. W. Joanne M. Willey, Linda M. Sherwood, *Prescott's Microbiology*. McGraw-Hill, 10th ed., 2016.

[9] B. Ma and R. Nussinov, "Enzyme dynamics point to stepwise conformational selection in catalysis," *Current Opinion in Chemical Biology*, vol. 14, no. 5, pp. 652 – 659, 2010. Nanotechnology and Miniaturization/Mechanisms.

[10] F. W. Dahlquist, "Remembering daniel e. koshland jr. (1920–2007)," *Protein Science*, vol. 16, no. 12, pp. 2583–2584, 2007.

[11] R. M. Daniel, M. E. Peterson, M. J. Danson, N. C. Price, S. M. Kelly, C. R. Monk, C. S. Weinberg, M. L. Oudshoorn, and C. K. Lee, "The molecular basis of the effect of temperature on enzyme activity," *Biochemical Journal*, vol. 425, no. 2, pp. 353–360, 2010.

[12] A. Wang, Q. Marashdeh, F. Teixeira, and L.-S. Fan, "20 - applications of capacitance tomography in gas–solid fluidized bed systems," in *Industrial Tomography* (M. Wang, ed.), Woodhead Publishing Series in Electronic and Optical Materials, pp. 529 – 549, Woodhead Publishing, 2015.

[13] D. Kunii and O. Levenspiel, "Chapter 1 - introduction," in *Fluidization Engineering (Second Edition)* (D. Kunii and O. Levenspiel, eds.), pp. 1 – 13, Boston: Butterworth-Heinemann, second edition ed., 1991.

[14] S. R. R. D. P. P. Roger G. Harrison, Paul W. Todd, *Bioseparations Science and Engineering*. Topics in Chemical Engineering, Oxford University Press, 2 ed., 2015.

[15] E. Tsotsas, T. Metzger, V. Gnielinski, and E.-U. Schlünder, *Drying of Solid Materials*. American Cancer Society, 2010.

[16] H. Wang, T. Dyakowski, P. Senior, R. S. Raghavan, and W. Yang, "Modelling of batch fluidised bed drying of pharmaceutical granules," *Chemical Engineering Science*, vol. 62, pp. 1524–1535, 03 2007.

[17] R. Stull, "Wet-bulb temperature from relative humidity and air temperature," *Journal of Applied Meteorology and Climatology*, vol. 50, no. 11, pp. 2267–2269, 2011.

Appendices

A

Select Model Constants and Variables

Parameter	**Symbol**	**Dimension**
Moisture content granules	X	kg/kg
Temperature air in	Tin	°C
Relative humidity air in	RH_in	%
Flowrate of incoming air	F	m^3/h
Initial temperature of solids	T	°C
Mass solids	solid	kg
Solids compensation factor	mass_solids	kg
Number unit steps	steplim	
Maximum relative humidity	RHlimit	%
Michaelis–Menten constant	n	
Michaelis–Menten constant	Km	
Michaelis–Menten constant	Rmax	
Michaelis–Menten compensation	R	
Wet-bulb temperature	T_w	°C
Vapour pressure at T_w	pwatTpw	Pa
Drying rate	dXdt	kg/unitstep
Temperature rate	dTdt	°C/unitstep
Relative humidity at drying rate	dRHd	%

B

Mathematical model

```
import numpy as np
import matplotlib.pyplot as plt
from scipy.integrate import odeint

Xp = np.linspace(0,1,100)
X = 0.153677569                 # Initial water content of solids
T = 60                          # Initial temperature of solids
RH_in = 0.03                    # Relative humidity of air in
x_air_in = 0.0077               # Moist cont. of air in
solid = 15                      # 15 kg for normal batches

mass_solid = solid / (2.1*1.16) # Compensation
# 2.1 * 1.16 for placebo
# 2.1 for Formulation B

# Luft
F = 700/3600                    # Initial flowrate of air
Tin = 90                        # Initial temperature of incoming air

steplim = 1500                  # num. of unit steps to peform
RHlimit = 0.5                   # Ma RH allowed

def granule_kinetics(Xp):
    # Calculates a normalised Michelis-Menten drying kinetics.
    # Will give r =1 until ish xp < 0.1 from whence it
    # (quickly) decreases.
    n = 2
    Km = 0.04                   # 0.05 for placebo
    Rmax = 1
    R = Rmax * Xp**n / (Km**n + Xp**n)
    return R

def wet_bulb_temperature(T,RH0):
    RH = RH0 * 100
    # Calculates the corresponding wet bulb temperature
```

```
    # of the particles
    Tw = T * np.arctan(0.151977*(RH+8.313659)**0.5) +
    np.arctan(T+RH)  - np.arctan(RH - 1.676331) +
    0.00391838*(RH)**(3/2) * np.arctan(0.023101*RH) - 4.686035

    return Tw*1.2

def temperature_kinetics(Tw):
    # Calculates the kinetic driving force from the wet bulb
    # temperaure. First approximates the vapor pressure of water
    # at Tw, then returns kinetic value at that point.
    # Kinetics derived from correlation between vapor pressure
    # at wet bulb temperature and drying rate at
    # constant rate period.

    pwatTpw = 10**(10.19625 - 1730.63 / (Tw + 233.426))

    return 0.0002*pwatTpw

def mass_n_heat_solver(Inpara,t,Rate):
    # Mass & Heat solver. Inputs rate from earlier
    # calculations.
    X = Inpara[0]
    T = Inpara[1]
    # Caluclates the drying rate of the particles,
    # from the combined_R, current X, and Xeq.
    dXdt = - 0.1 * (Rate)
    # Creates a global variable and saves dXdt,
    # for use in calculation of RH

    global dXdt_data
    dXdt_data = dXdt
    # Calculates the change in temperature as a function of
    # the drying rate, which in turn is calculated
    # from dxdtsolver

    dTdt = ((Tin * 1 * F - T * 1 * F) + dXdt *4200 *mass_solid) /
           (F * 1 + mass_solid * 0.3981 * (1 - X)
           + mass_solid*X*4.2)

    return [dXdt, dTdt]

def moisture_content_air(x_out,t,dXdt):
    # Calculates the corresponding relative humidity at the
    # earlier calculated evaporation rate, and T.

    dX_air_dt = (x_air_in - x_out) - dXdt * mass_solid / F
```

```
    return dX_air_dt


def antoines_equation(T):
    # Calculates the vapor pressure of water at
    # the input temperature
    A = 10.19625
    B = 1730.630
    C = 233.426

    return 10**(A-B/(C+T))

def relative_humidity_function(RH,t,x_air,T):
    # Calculats the relative humidity as a function of
    # moisture content, current RH and T
    ant = antoines_equation(T)

    RH_air_in_to_x = RH_in * ant * 0.62
                     / (101325 - RH_in * ant)

    RH_current_to_x = RH * ant * 0.62 / (101325 - RH * ant)

    vapor_pressure_water = (RH_air_in_to_x - RH_current_to_x +
          x_air)*101325 /(0.62 + RH_air_in_to_x -
          RH_current_to_x + x_air)

    dRHdt = vapor_pressure_water / ant

    return dRHdt

#%% Rate Calculations

t = np.linspace(0,steplim,steplim+1)

for i in range(len(t)-1):
    tspan=[t[i], t[i+1]]

    granule_rate = granule_kinetics(X)
    # Calculates the rate from the granule_kinetics correlation

    wet_bulb_T = (wet_bulb_temperature,T,RH)
    wet_bulb_rate = temperature_kinetics(wet_bulb_T[1])
    while True:
        drying_rate = granule_rate * wet_bulb_rate
        # Calculates a combined drying rate from
        # wet_bulb_temperature & granule_kinetics

        #%% Mass & Heat Calculations
```

```
Inparam = [X, T]
mass_n_heat = odeint(mass_n_heat_solver, Inparam,
              tspan, args=(drying_rate,))

Xkan = mass_n_heat[1,0]
Tkan = mass_n_heat[1,1]

RhMaxAllowed = 0.2275*np.log(Xkan) + 1.3137
if Xkan < 0.006:
    RhMaxAllowed = 0.1
X_air_sol = odeint(moisture_content_air, X_air, tspan
            , args=(dXdt_data,))
X_air = X_air_sol[1]

RH_sol = odeint(relative_humidity_function, RH, tspan
       , args=(X_air, Tkan))
RHkan = RH_sol[1]
if RHkan >= RhMaxAllowed:
    granule_rate = granule_rate * 0.99
elif RHkan < RhMaxAllowed:
    break
```

C

Code Documentation

Pilot Scale Fluidised Bed Dryer Model – Documentation

Edvin Ingmarsson

August 2019

1 Introduction

The purpose of this document is to explain how to use the mathematical model developed as part of the master thesis "Kinetic modelling and simulation". The models purpose is to accurately simulate and predict the drying progress in a pilot scale fluidised bed dryer. The document describes how to initialise the model and how to extract data to an .csv file.

2 Usage

This section describes how to initialise the model, input process parameters and conditions.

2.1 Initialisation

In order for the model to run some parameters have to be defined. Namely these are:

- Temperature of air in
- Relative humidity of air in
- Flowrate of air in
- Operating temperature dryer
- Initial moisture content granules
- Initial batch mass
- Desired unit steps
- Formulation
- Enzyme type
- Enzyme loading

These process parameters and conditions allows the model to take the current conditions into account and accurately model the drying. The parameters in the model are in the code (Appendix A) described, hence no further explanation of them is given.

2.2 Simulation

After the process parameters and conditions have been defined the model can be started. The time required to run the model differs slightly depending on the conditions and the computer used. However a typical simulation should not require more than 3 minutes.

If the time for simulation is to long, the value in RH-check can be adjusted. The standard value is 0.99. To decrease the simulation time this value can be decreased. However the decreased computational time is traded for lower accuracy. Hence it is recommended that the value is kept at 0.99.

At each unit step vital values are stored in an array. These are used for visualising of the results after completing the calculations.

2.3 Evaluation of results

When the model has performed the number of unit steps defined the model stops. A selection of parameters are then displayed in a graph as a function of time. As standard these are: Moisture content in granules, solids temperature, relative humidity and drying rate.

3 Data Extraction

When the simulation is completed large datasets are stored in arrays. In these the temperature, granule moisture content, drying_rate, granule_rate, dXdt and the relative humidity is stored for each unit step.

In the corresponding thesis the plots were created in R with ggplots. To extract the data from Python the following command was used:

```
np.savetxt("FileName.csv", np.column_stack((unitsteps,
Array)), delimiter=",", fmt='%s')
```

With 'FileName.csv' being the name of the created file with the data sets 'unitsteps' and 'Array'. 'Array' can be any of the data arrays mentioned above.

Subsequently the data was imported in R and further processed.